EUMETSAT
Monitoring weather and climate from space
Surveiller le temps et le climat depuis l'espace

SALGEE

Synoptic and climatic aspects of fire activity and emission effects

Christo Georgiev

National Institute of Meteorology and Hydrology, Bulgaria

Part I: Characterizing fire activity in Eastern Mediterranean part of Europe by surface temperature and soil moisture variability

J. Stoyanova, C. Georgiev, P. Neytchev, A. Kulishev

Part II: Identification of ozone production from wildfire emissions by using IASI measurements

C. Georgiev, A. Karagiannidis, J. Prieto

7th SALGEE Virtual Workshop "Drought & Vegetation Monitoring: Energy–Water Cycle"
24 – 26 Nov 2021

EUMETSAT
Monitoring weather and climate from space
Surveiller le temps et le climat depuis l'espace

SALGEE

CHARACTERIZING FIRE ACTIVITY IN EASTERN MEDITERRANEAN PART OF EUROPE BY SURFACE TEMPERATURE AND SOIL MOISTURE VARIABILITY

Julia Stoyanova, Christo Georgiev, Plamen Neytchev, Andrey Kulishev

National Institute of Meteorology and Hydrology, Bulgaria

7th SALGEE Virtual Workshop "Drought & Vegetation Monitoring: Energy–Water Cycle"
24 – 26 Nov 2021

Introduction

Climatic anomalies and related fire activity

- **Variability of climate is a major driver of fire in terrestrial ecosystems that influence fire regimes (Bradstock, 2010).**
- **Climate variability is connected to fires at two distinct temporal scales (Hessl, 2011).**
  - **Short-term climatic anomalies (months to years) affect fires by modifying vegetation growth and fuel moisture before the fire and by influencing weather during the period of fire spread.**
  - **Long-term (decadal or longer) indirect effects on the distributions of major vegetation types and their functioning that in turn constrain the landscape-scale mosaics of fuels and vegetation.**

Outline

Focus: Quantification the vulnerability to biomass burning across the climatic gradient for Eastern Mediterranean Europe using satellite data and products, ground observations and modeling of land surface state. Identification of fire-risky areas is important for the purposes of mitigation activities because vegetation biomass burning in the region is not only a natural hazard and can also be a climate change driver.

Objectives:

- **To study drought and related fire vulnerability over Bulgaria applying relevant concepts/indexes.**
  - **To assess vegetation water stress in relation to the fire activity.**
  - **To perform climatic analyses of fire activity in relation to drought occurrence for identification of drought-prone areas on a regional basis.**

Research approaches and Data sets

1) **Satellite monitoring of Fire detections and Biomass burning effects.** **Data set: LSASAF (FRP)-PIXEL (Wooster et al., 2015, (2004-2019) .**
2) **Analyses of biogeophysical indicators and their dynamics in long-term aspect.**
   - **Soil Moisture Availability (SMA) to the Vegetation cover, based on SVAT modeling (Stoyanova and Georgiev, 2013). SMA Index (SMAI) in 6-level scale, operational daily derived at NIMH since 2007.**
   - **Land surface temperature retrieval from IR satellite measurements. Data set: LSASAF LST, Jun-Sep (2007-2018).**
   - **Temperature difference of LST – air temperature (LST-T2m) . Data set: LSASAF LST and Air temperature at SYNOP network .**
3) **Correlation analyses of fire activity and biogeophysical indexes for different Land cover types.**
4) **Quantitative comparative analyses for climate-fire relations.**
5) **Trend analyses.**

STANDPOINTS

- **Different fire regime components (occurrence, size/severity) exhibit characteristic spatial/temporal patterns that reflect differences and variations in biophysical drivers of the related physical and environmental processes.**
- **Knowledge about fire-climate relations on a regional scale is important to define risky regions and periods as well as for projection the effects of global environmental change.**

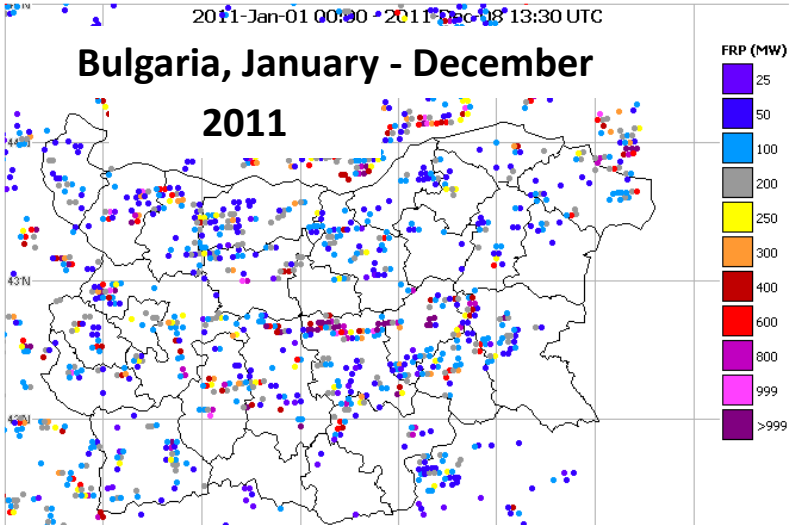

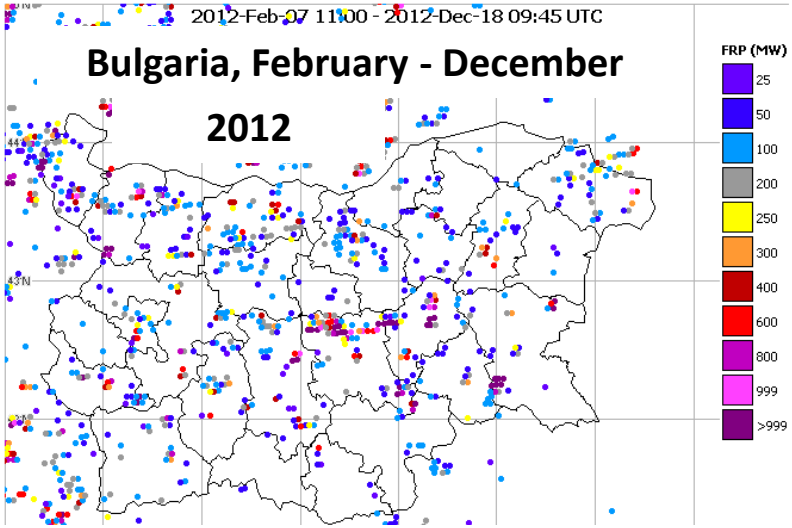

<u>Bulgaria as a fire-prone area</u>: Examples based on LSASAF Fire Radiative Power FRP-Pixel product (radiant energy released during biomass burning)

1. Characterizing fire activity: Use of LSASAF FRP-Pixel product based on SEVIRI observations

MSG FRP-Pixel product's efficacy and reliability to reflect the fire activity is evaluated towards the course of monthly accumulated forest fire activity (2007-2017) reported by ground observations of Executive Forest Agency (EFA) of Bulgaria.

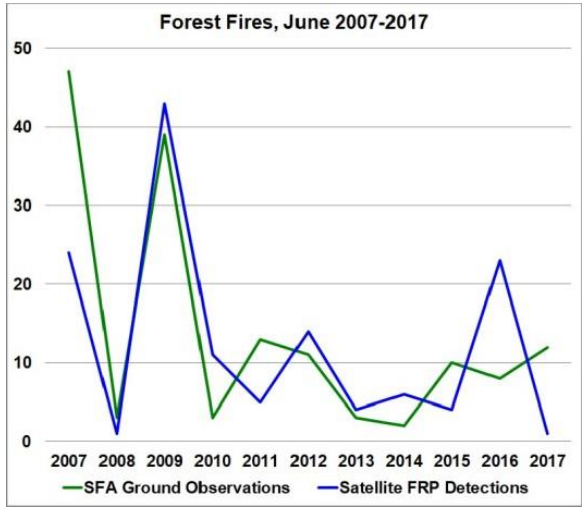

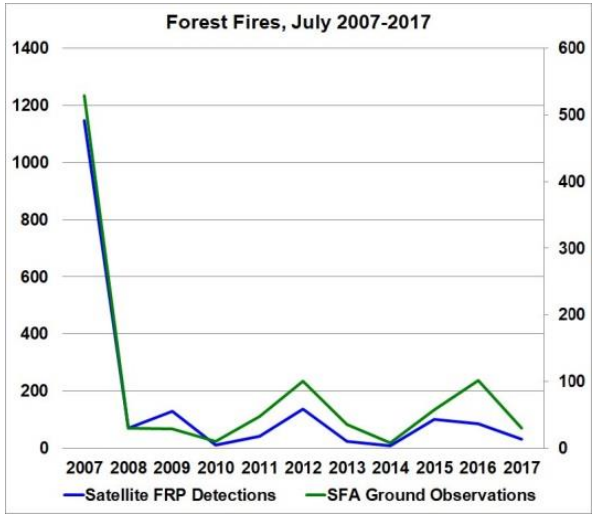

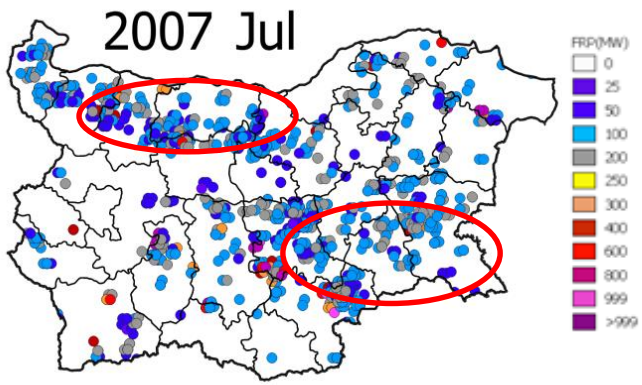

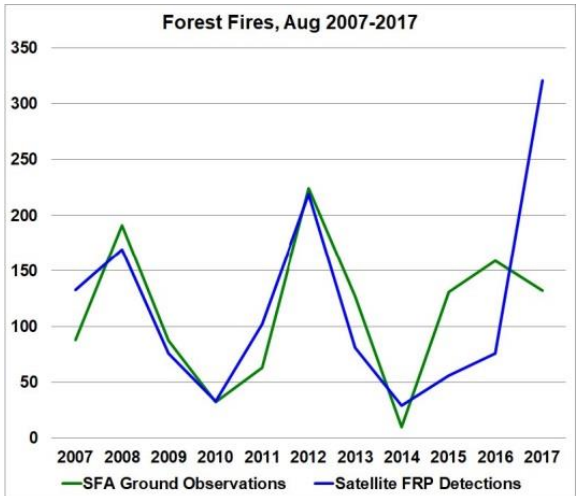

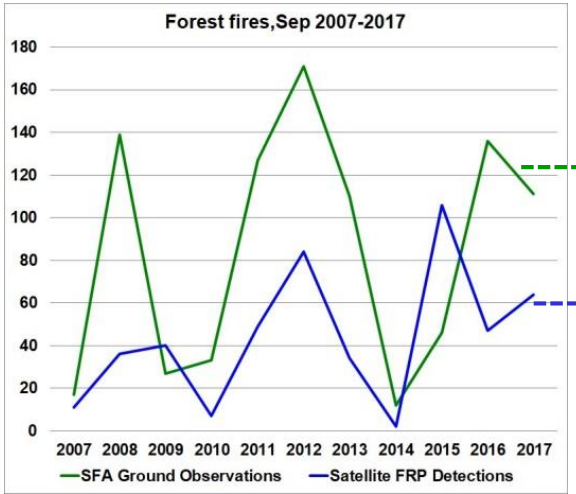

Forest fires from EFA Ground observations

Satellite Fire detections by LSA SAF FRP-Pixel Product

Accumulated LSASAF FRP-Pixel detections over Bulgaria, Monthly maps

Jun-Sep of *2004-2019 period*

Total Jun-Sep

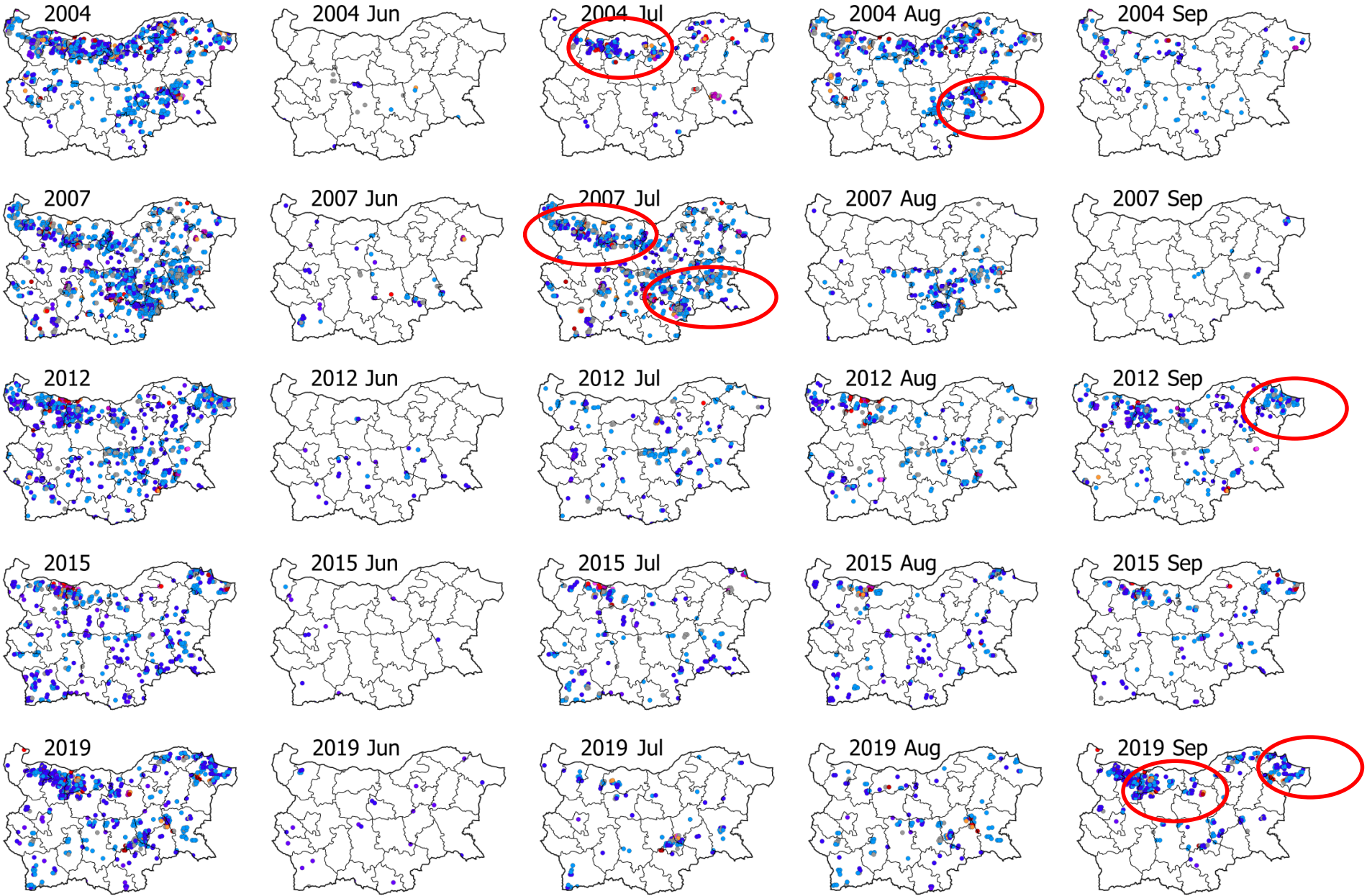

Spatial distribution of fire activity at opposite weather/climate anomalies

Meteosat FRP (MW) energy released from biomass burning

- **„Heat maps“ of FRE released from biomass burning for characterizing geographic clustering of fire activity over Bulgaria in extreme dry and wet climatic anomalies.**

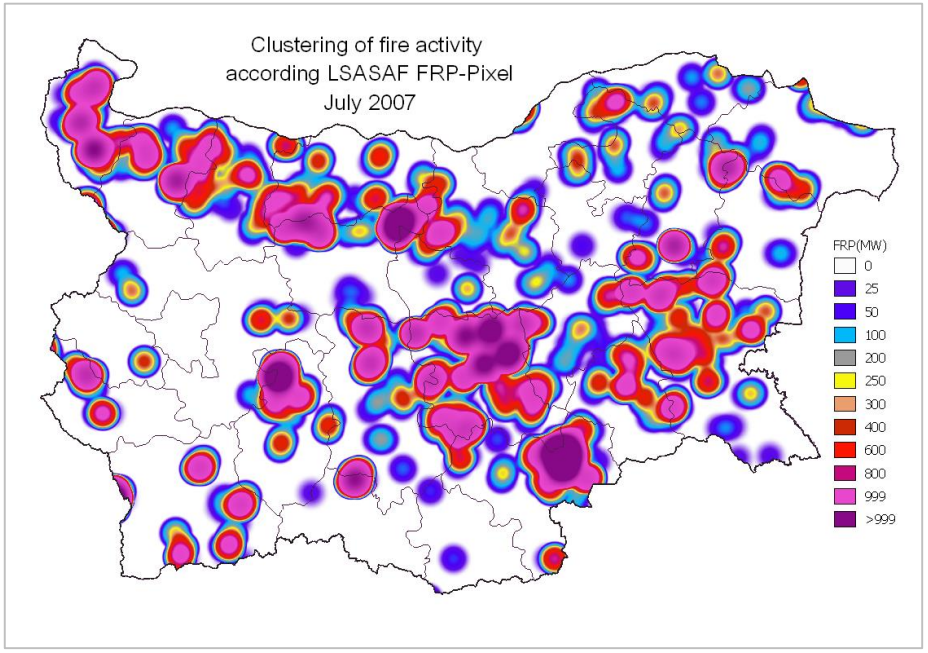

2007, extreme fire occurrence at a strong warm & dry climate anomaly: Satellite FRP product indicates very high fire energy released.

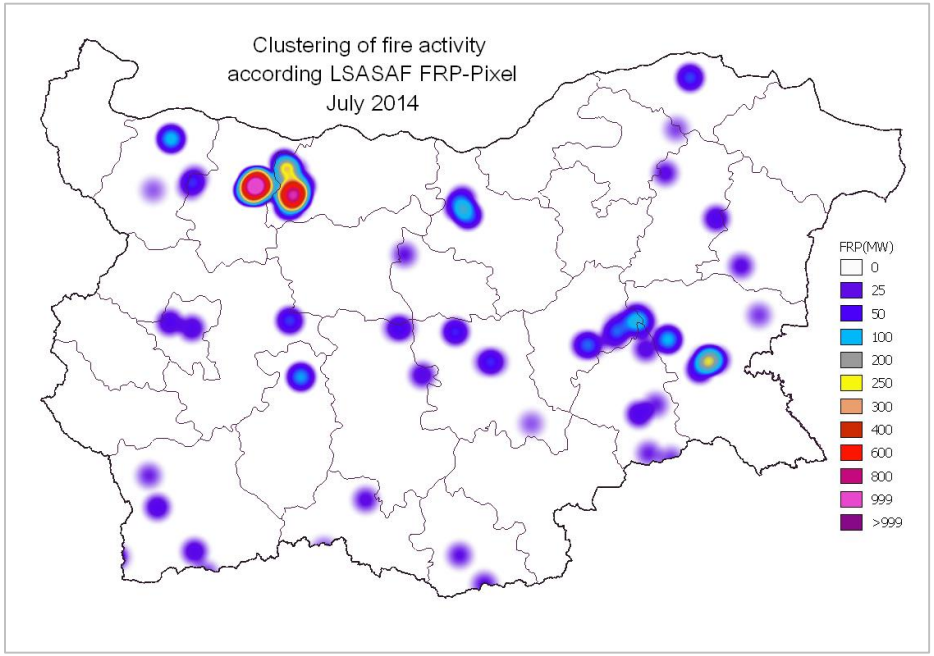

2014, low fire activity at a strong cool/wet climate anomaly: Satellite FRP product indicates very low fire energy released.

2. Physical aspects of fire activity: Spatial distribution of LST as a biogeophysical parameter along with FRP detections

- **Mean monthly anomalies of LSASAF LST and FRP fire detections mapped.**

2007

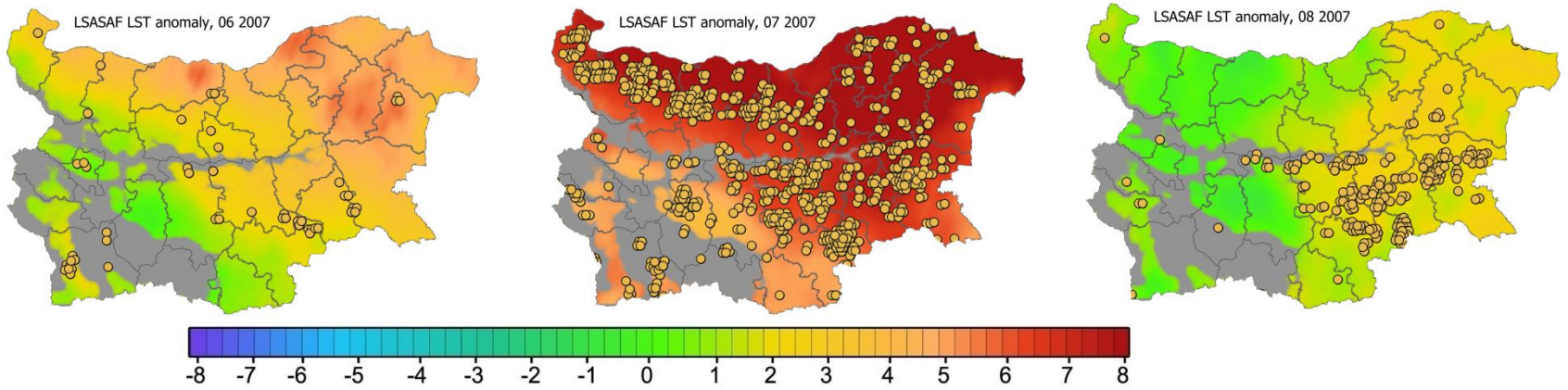

2014

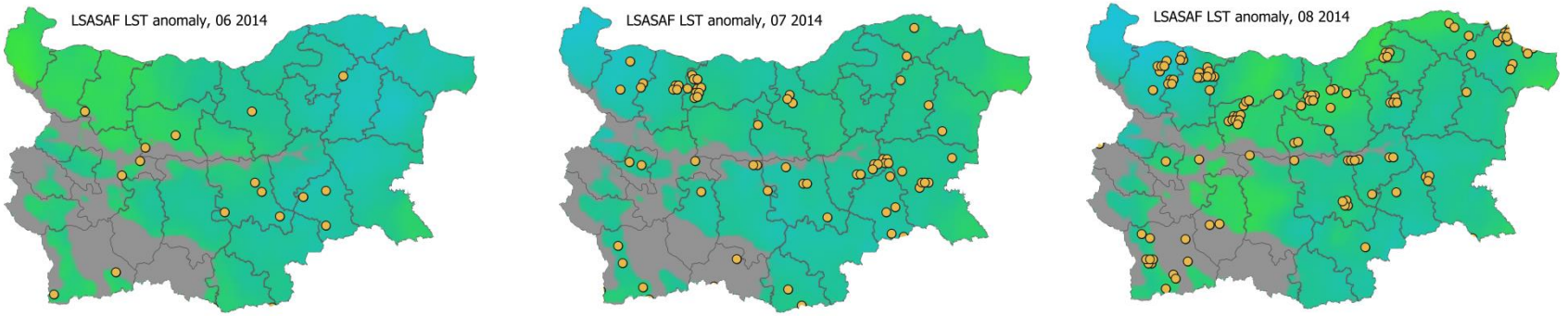

- **The higher positive LST anomalies correspond to higher number of detected fires**
- **Both being maxima in the extreme heatwave over SE Europe in July 2007,**
- **and minima in 2014 with a strong cool/wet climate anomaly**

Physical aspects of fire activity: Spatial distribution of SVAT model derived SMA biogeophysical Index along with FRP detections

- **SMA mean monthly anomalies with overlaid FRP fire detections.**

2007

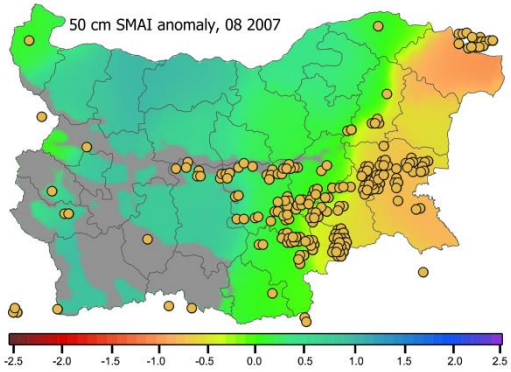

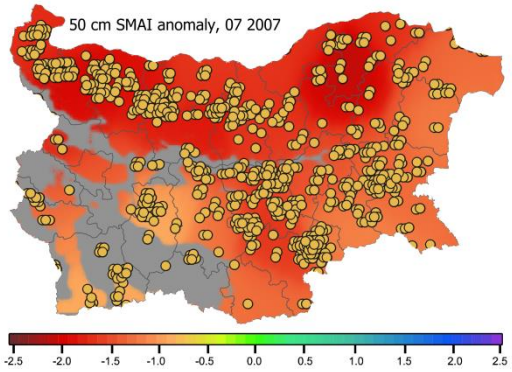

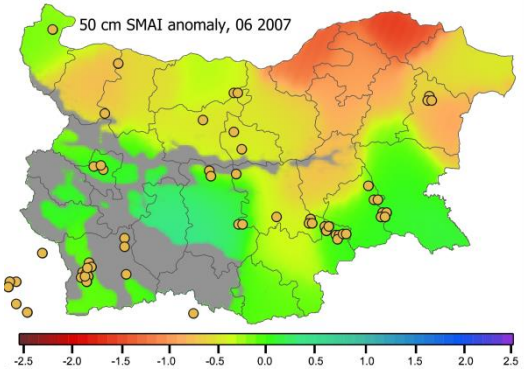

2010

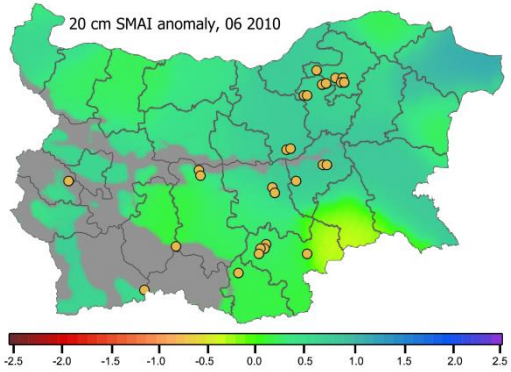

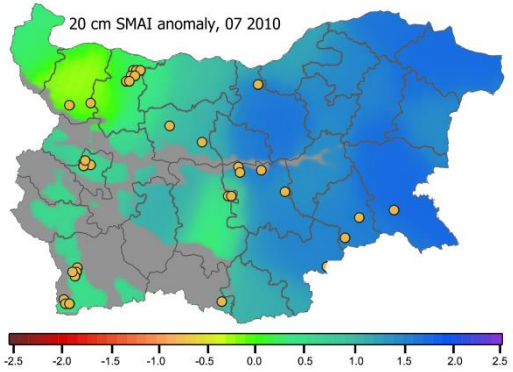

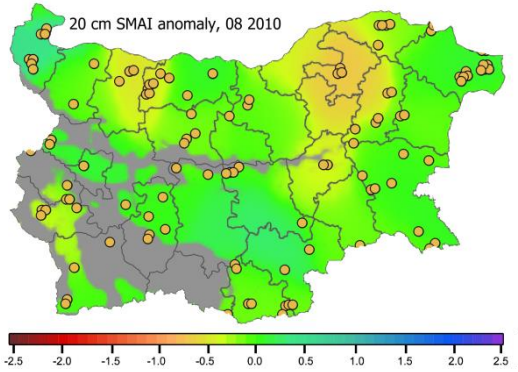

The amount of fire occurrence is related to the strength of negative SMA anomalies.

- The stronger negative SMA anomalies are related to higher number of fire detections:

- being extremely high in July 2007 with a strong dry/warm climatic anomaly.

- Low fire activity in 2010 corresponds to low negative or positive SMA anomaly at 20-50 cm soil depth.

3. Temporal variability of LST parameters vs. fire activity: Jul-Sep (2007-2018)

a)

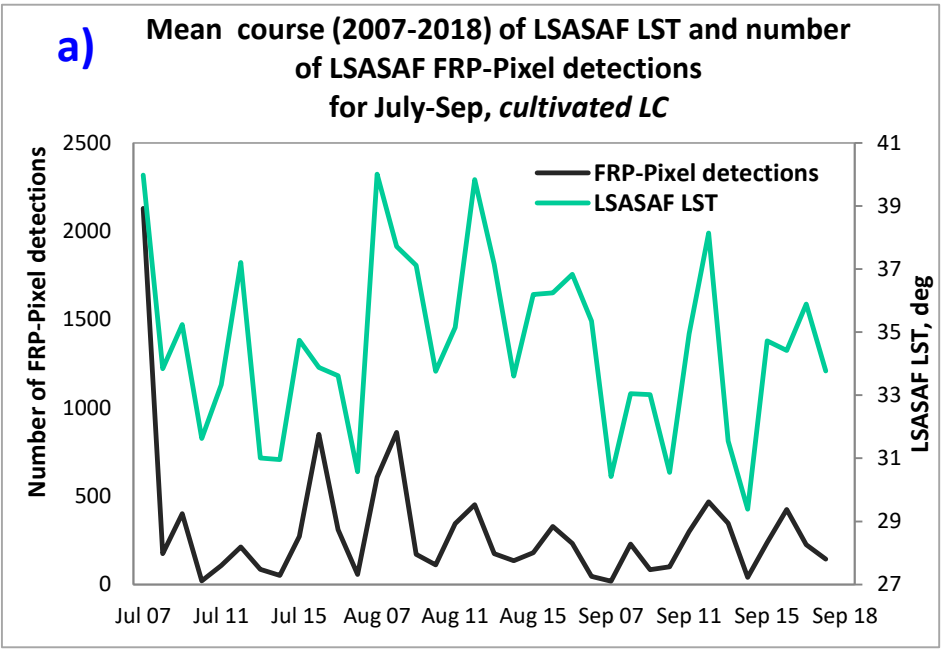

- **Cultivated LC type**

Synchronized behavior in mean (2007-2018) seasonal (Jul-Sep) courses of:

a) LST and Number of fire detections

b) LST and Total FRP released (MW)

c) (LST-T2m) and Total FRP released (MW)

b)

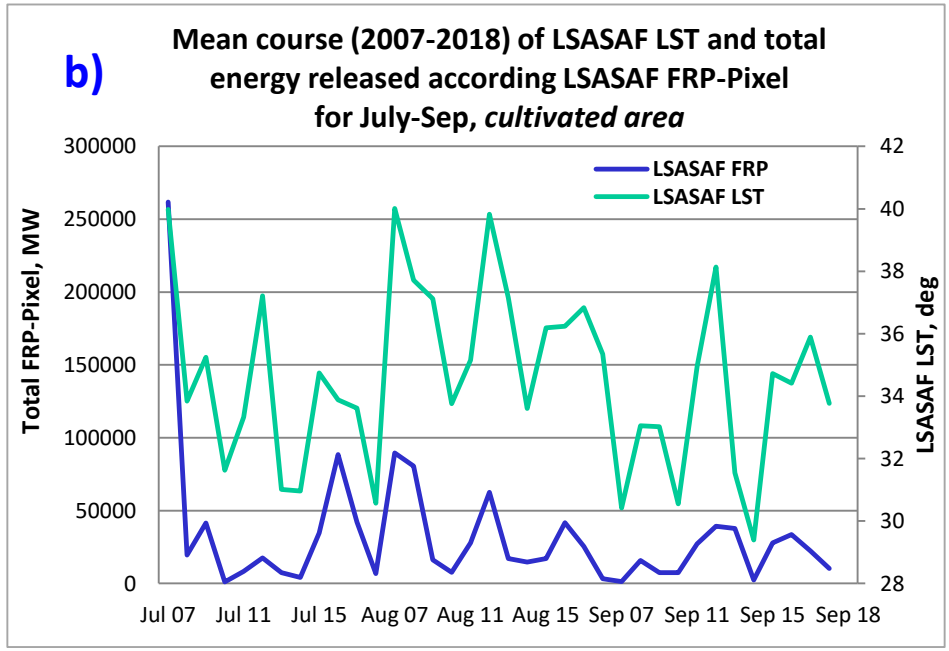

c)

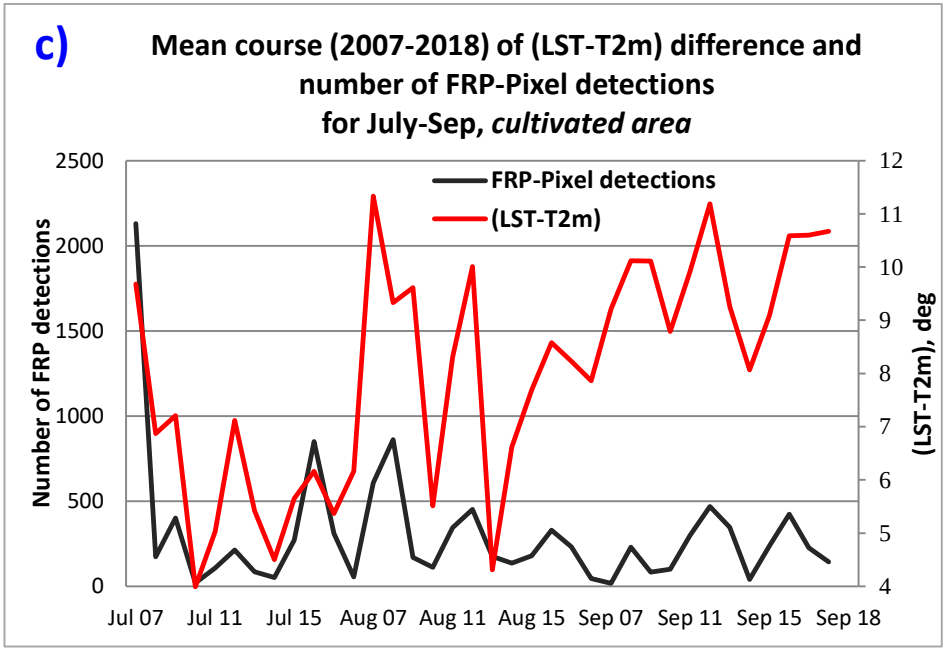

a)

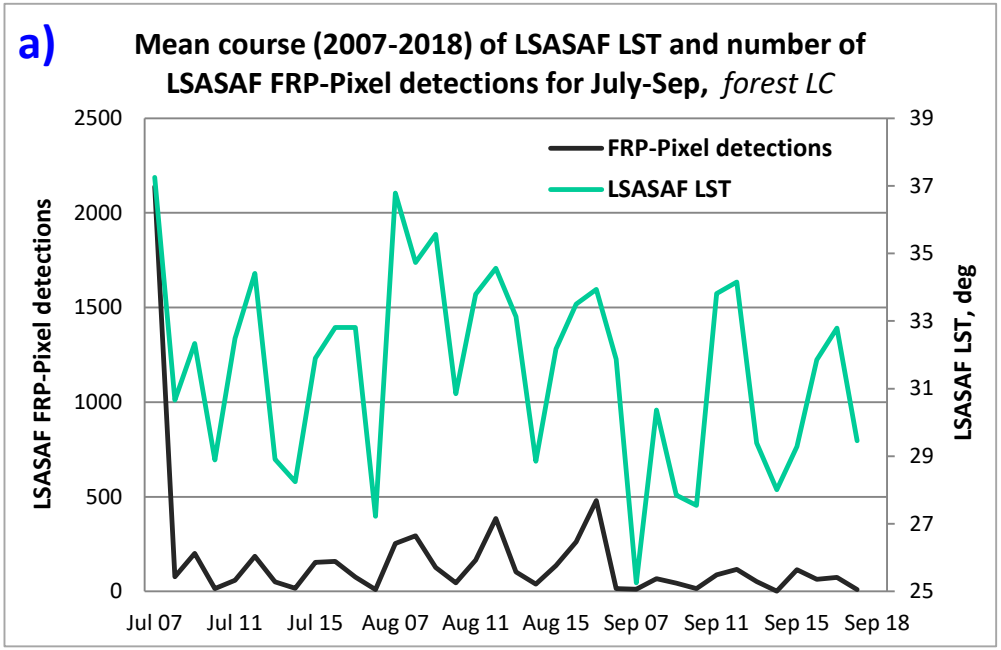

Temporal variability of LST vs. biomass burning effects: Jul-Sep (2007-2018)

- **Forest LC type**

Synchronized behavior in mean (2007-2018) seasonal (Jul-Sep) courses of:

a) **LST and Number of FRP detections at forest LC types**

b) **LST and Total FRP (MW) radiant energy released by burning of forest biomass**

- **Increase of LST is related to corresponding increase of the number of forest fires (detections by LSASAF FRP-Pixel) and the radiant energy released from biomass burning.**

b)

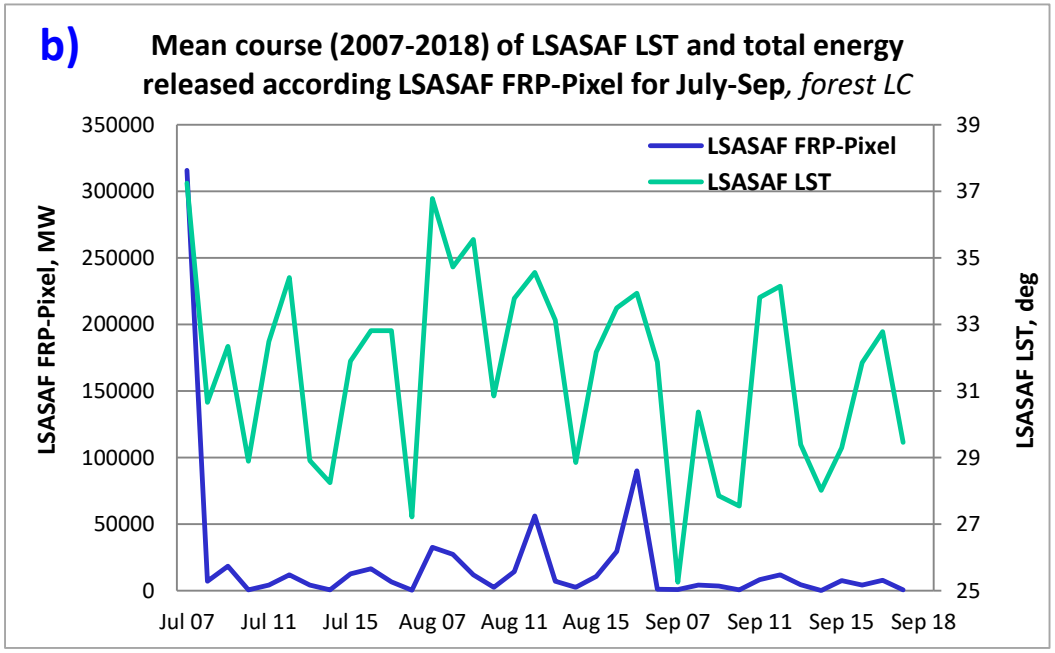

Correlation analyses: Fire activity vs. monthly mean LST /LST anomalies

Increasing exponential model fits the relations for all LC types at high correlation and significance level (p)

Total FRP accumulated yearly over 2007 – 2018 period

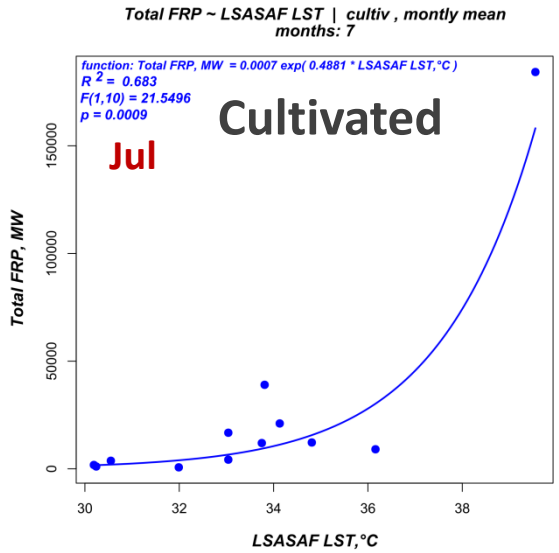

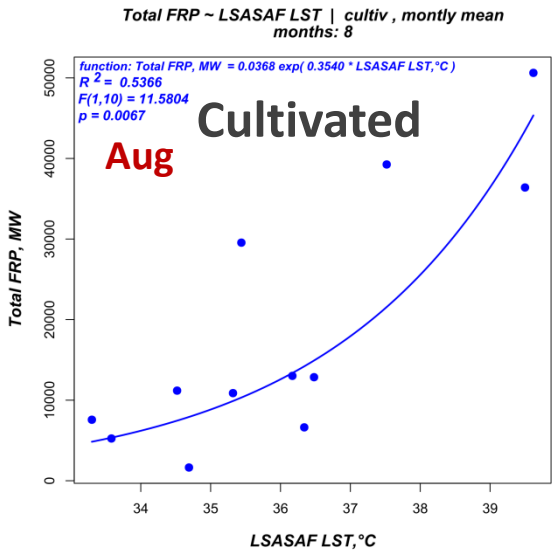

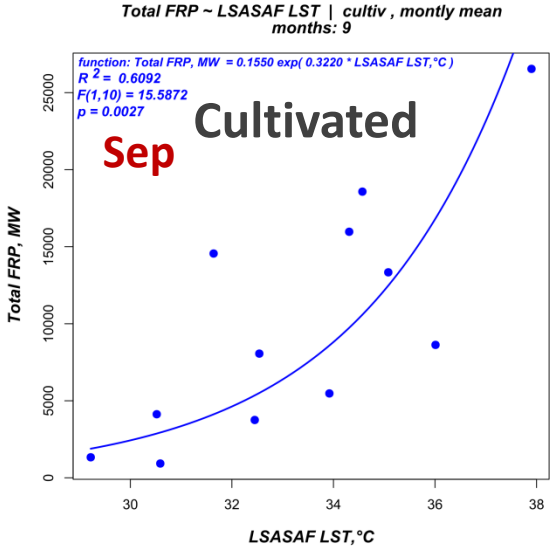

LSASAF FRP-Pixel (MW) vs. LSASAF LST

	Forest R^2	Cultivated R^2	Shrubs R2
	FRP (MW) vs. LST	FRP (MW) vs. LST	FRP (MW) vs. LST
Jul	0.772	0.683	0.593
Aug	0.407	0.537	0.481
Sep	0.436	0.609	0.432

LSASAF FRP detection vs. LSASAF LST anomaly

	Forest R^2	Cultivated R^2	Shrubs R^2
	Fires vs. LSTanom	Fires vs. LSTanom	Fires vs. LSTanom
Jul	0.831	0.675	0.634
Aug	0.761	0.565	0.454
Sep	0.630	0.671	0.531

Fire activity vs. monthly mean SMAI anomalies for different LC Types:

Decreasing exponential model fits the relations for all LC types at high correlation and significance level (p)

Total FRP accumulated yearly over 2007 – 2018 period

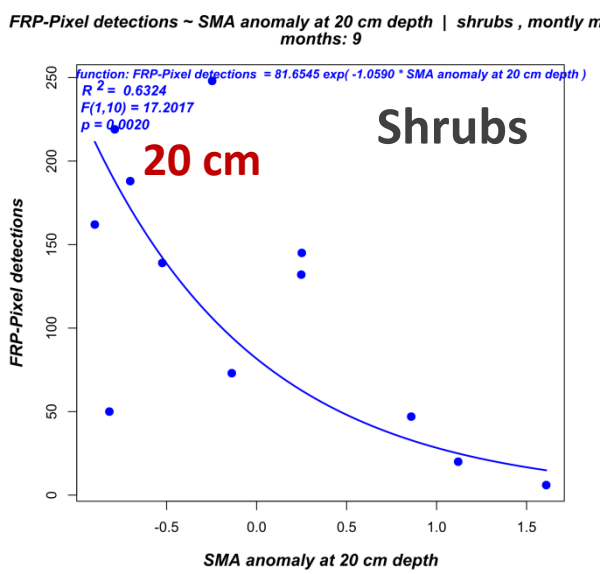

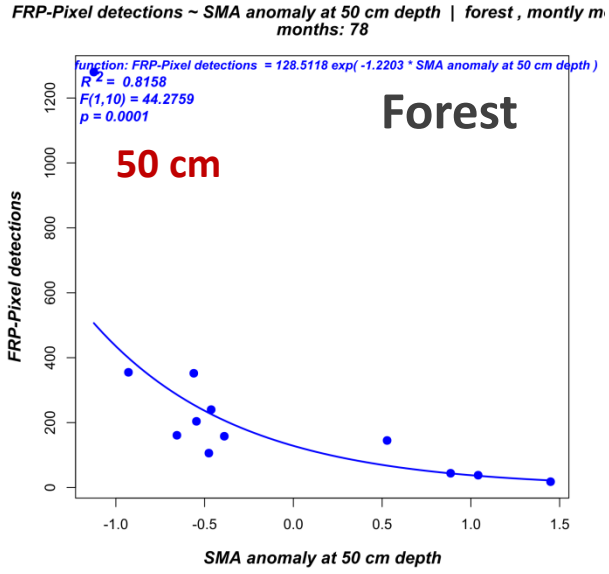

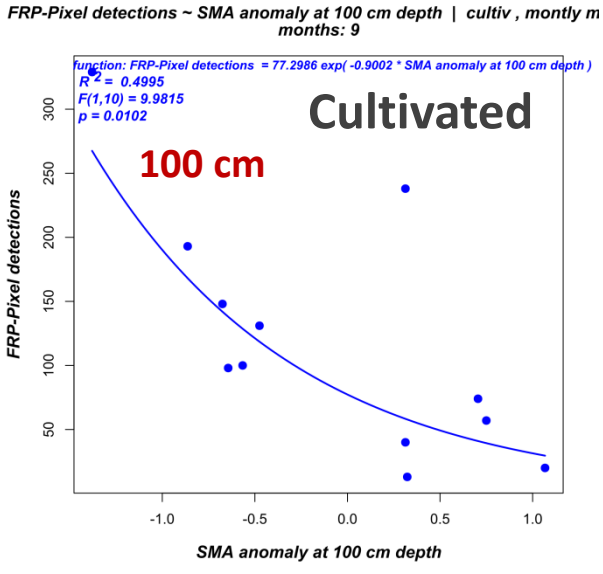

LSASAF FRP (MW) vs. SMAI anomaly at 20 cm

	Forest R^2	Cultivated R^2	Shrubs R2
	FRP vs. SMAI 20cm	FRP vs. SMAI 20cm	FRP vs. SMAI 20cm
Jul	0.715	0.665	0.423
Aug	0.338	0.172 ns	0.113 ns
Sep	0.002 ns	0.547	0.225

LSASAF FRP-Pixel detections vs. SMAI anomaly at 50 cm

	Forest R^2	Cultivated R^2	Shrubs R^2
	Fires vs. SMAI 50cm	Fires vs. SMAI 50cm	Fires vs. SMAI 50cm
Jul	0.884	0.713	0.523
Aug	0.512	0.524	0.444
Sep	0.02 ns	0.816	0.645

Statistical analyses of the relation between fires & biogeophysical drivers related to LST

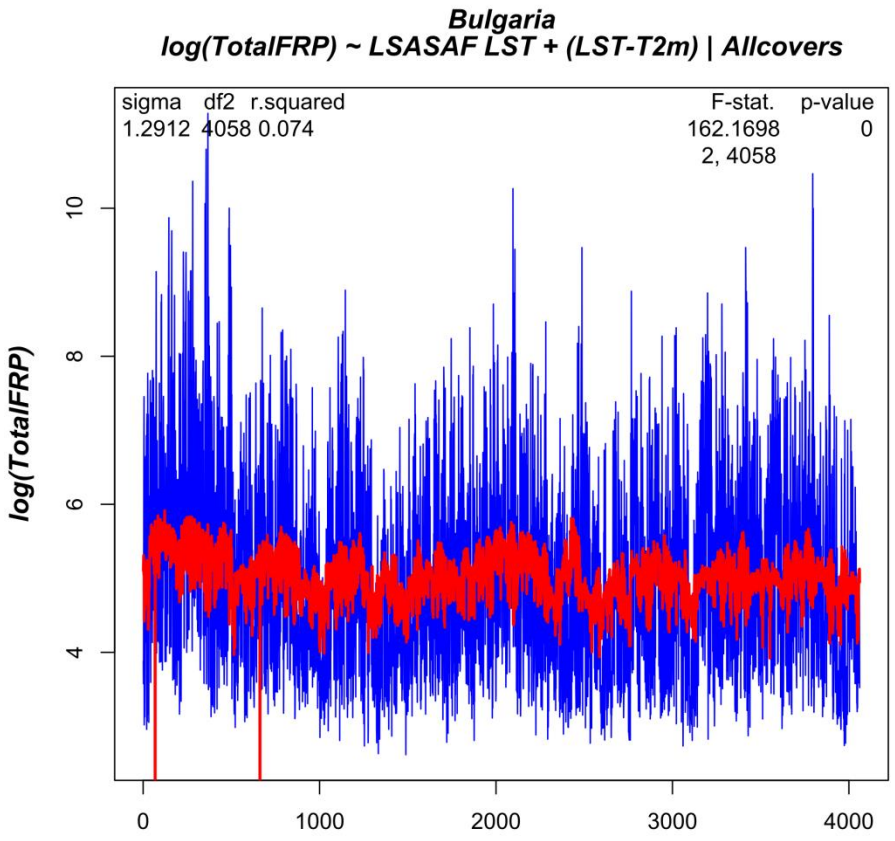

Blue – Observations (FRP-Pixel detection)
Red – Model (fitted data)

1. Generalized linear statistical model

- **A generalized linear model for description of Fire Radiative Energie (FRE) released from biomass burning is constructed.**
- **The logarithmic model uses as predictors: LSASAF LST and (LST-T2m).**
- **There is a good fit in the trend of variability between the released FRE from satellite detections and the generalised linear model.**
- **This trend of similarity is preserved for each LC type : forest, shrubs, cultivated, considered separately.**
- **The model is intended to evaluate the imput of selected predictors of fire activity, not to be an exact quantification of FRP (MW).**

Estimation procedure: package "lm" from R project, see: ***R Core Team (2016). R: A language and environment for statistical computing. R Foundation for Statistical Computing, Vienna, Austria. URL https://www.R-project.org/.***

Fire activity spatial distribution & Trend analyses

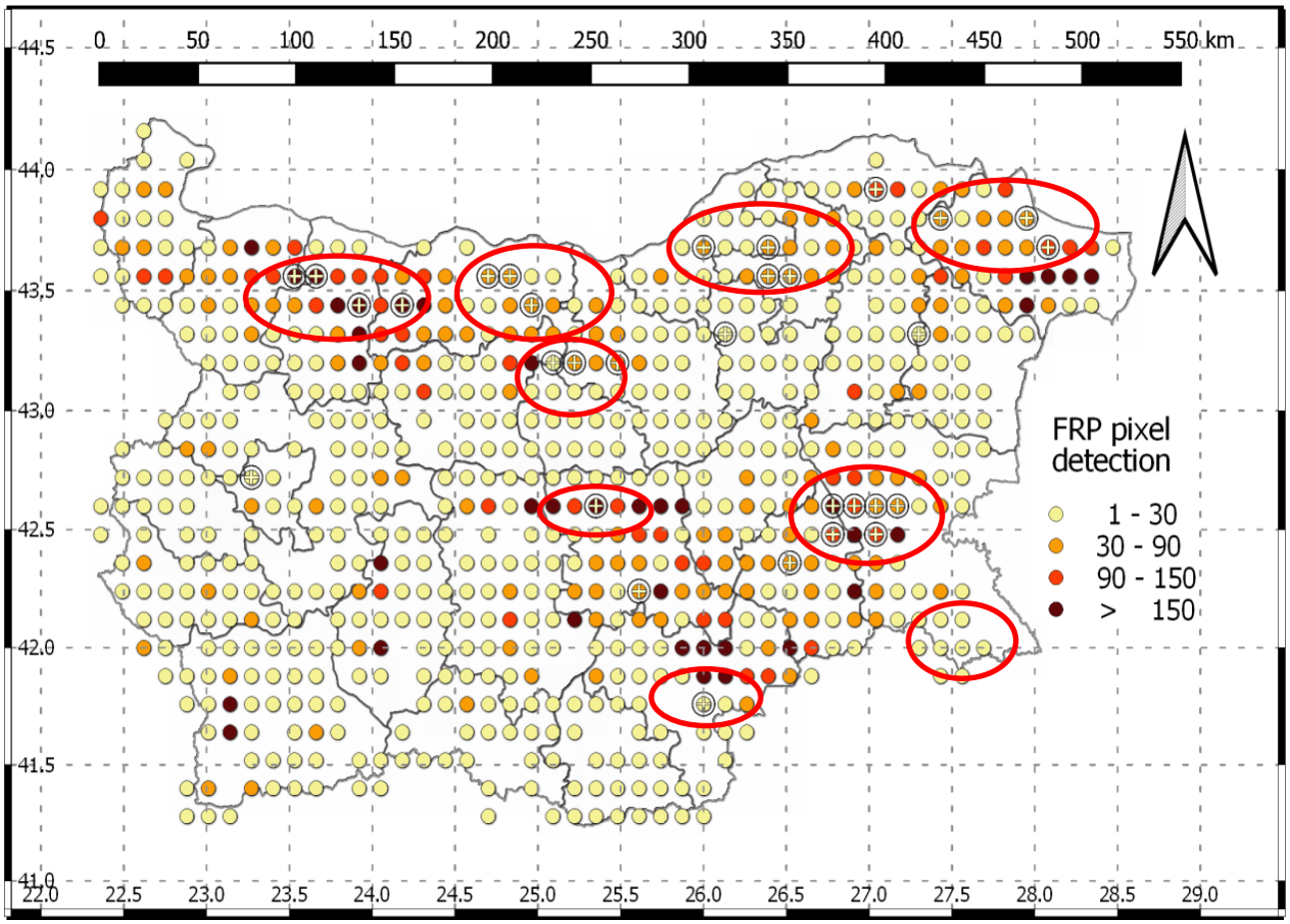

Accumulated number of fire detections by the LSASAF FRP-Pixel product during 2007–2018 period (Jun-Sep).

- **The spots of higher fire activity are identified.**
- **Regions of statistically significant positive trend in fire activity are localized.**

The fire number is the sum of fire detections in each MSG pixel over Bulgaria (4-5 km^2 resolution) resampled within areas of 100 km^2 (10 km x 10 km).
The sign "+" indicates positive trend (passed the Mann–Kendall significance test at the 5% level).

5. Concluding remarks

- **Climatic analyses of wildfire occurrence and radiant energy released are performed in the view of the variations in biophysical drivers of the related physical and environmental processes over Bulgaria (Eastern Mediterranean).**
  - **Long-term (2007-2018) LSASAF LST data is used to derive monthly mean land surface temperature for use as a fire risk.**
  - **As a reference in drought assessment, Soil Moisture Availability to vegetation derived through meteorological 'SVAT_bg' model is used.**
  - **Long term (2004-2019) LSASAF FRP-Pixel data provides information on the spatial-temporal wildfire distribution in the most risky period (Jul-Sep).**
- **Results:**
  - **Increasing exponential model fits the relations Fire activity vs. mean monthly LST /LST anomalies for different LC Types.**
  - **Validity of this approach is confirmed by the result that the relation Fire activity vs. mean monthly SMA anomalies is described by decreasing exponential model for all LC types.**
  - **A generalized linear statistical model fits the relationship between LST (*as a predictor*) and the released energy from biomass burning (Total FRP, MW), showing that satellite LST can be a source of information in the climatic fire risk assessments.**
  - **Regions of statistically significant positive trend in fire activity can be localized.**

IDENTIFICATION OF OZONE PRODUCTION FROM WILDFIRE EMISSIONS BY USING IASI MEASUREMENTS

Christo Georgiev[1], Athanasios Karagiannidis[2] Jose Prieto[3]

[1]NIMH of Bulgaria,

[2]IERSD, National Observatory of Athens, [3]EUMETSAT

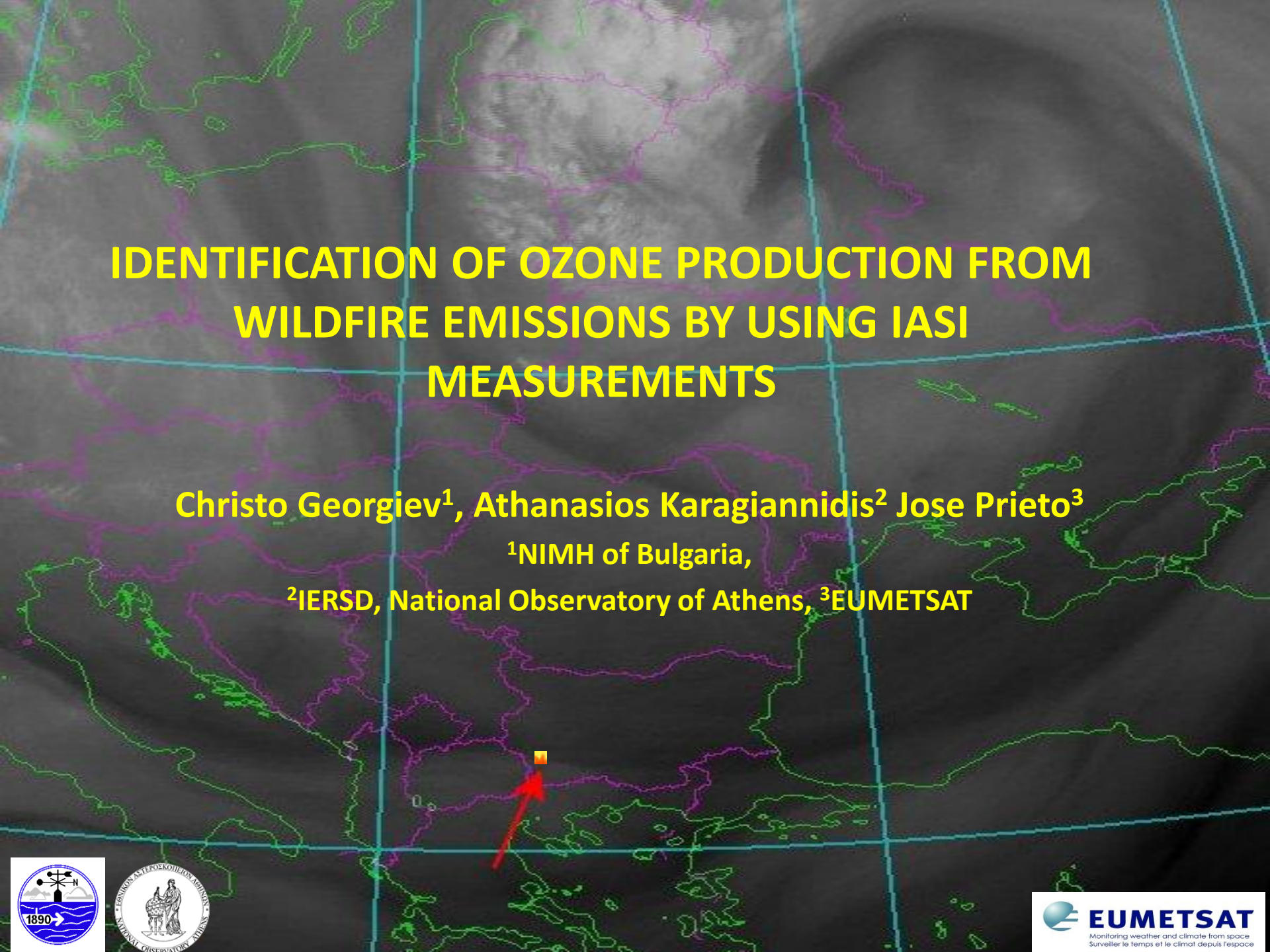

EUMETSAT
Monitoring weather and climate from space
Surveiller le temps et le climat depuis l'espace

Outline

- **Focus:** **Ozone production from wildfires: Forest fire plumes are rich in primary pollutants (such as particles, carbon monoxide, non-methane volatile organic compounds and nitrogen oxides). Photochemical transformations of those pollutants can produce secondary ones, including ozone (Rubio et al., 2015). Tropospheric ozone (O_3) negatively impacts human health and ecosystems, being also a greenhouse gas.**
- **Aim:** **To examine the sensitivity of ozone retrievals from IASI measurements on board of Metop satellites to low-level ozone production in close vicinity of wild fires.**
- **Challenges:** **Uncertainties and complexity in studying the ozone production from wildfire plumes due to various mechanisms that influence the near-surface ozone concentrations.**

The problem of ozone impacts from wildfires areas

Demonstrating and quantifying the ozone impacts from wildfires areas is challenging (see Jaffe and Wigder, 2012).

- **Ozone, as a secondary pollutant, peaks only downwind of the fire location.**
- **While most pollutants emitted by a wildfire decrease with distance, ozone can increase.**
- **The wind around a fire region can vary significantly and the fire emissions in an aged plume may change direction of propagation.**
- **Complexities are also due to upper troposphere dynamics: Strong increase of fire activity is very often due to deep stratospheric intrusions that also cause transport of O_3 to the earth surface and mix it with the effect of O_3 production in the fire plume.**

Stratospheric intrusion seen in WV imagery and increased fire activity

Surging dry dark slot in WV imagery

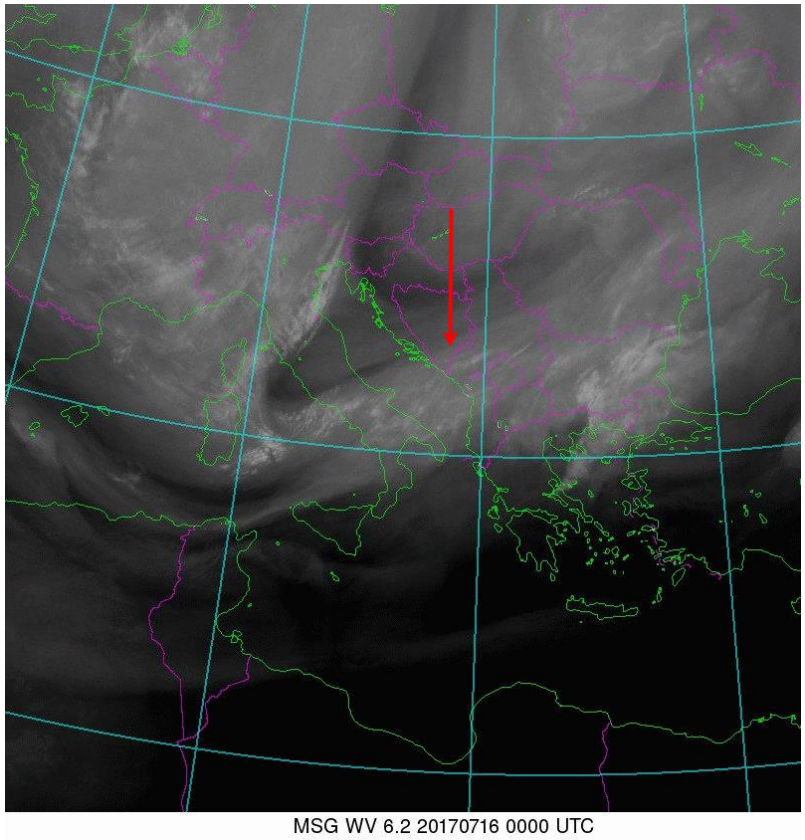

MSG WV 6.2 20170716 0000 UTC

Fire detections by LSA SAF FRP PRODUCT

15 - 16 July 2017

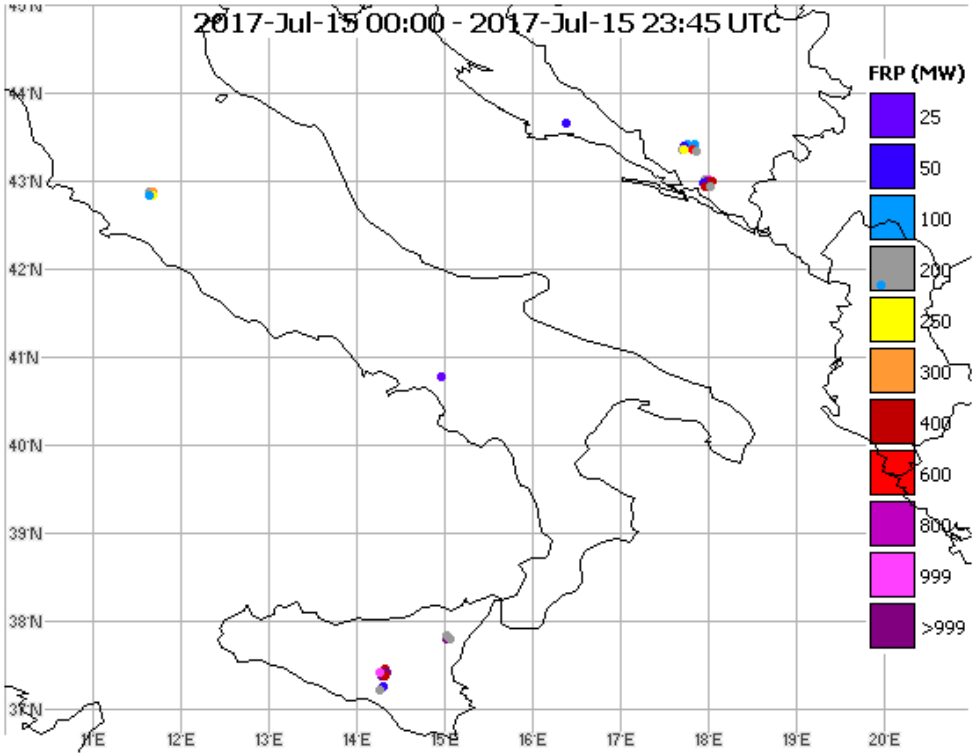

A deep tropopause folding is associated with column of high, fast moving, dry, ozone-rich air that descends rapidly to or near the Earth's surface.

This stratospheric dry intrusion affects surface drying and intensifying the winds, thus causes abrupt fire developments (Mills 2008; Zimet et al. 2007; Fox-Hughes, 2015).

Deep stratospheric intrusion seen in retrieved by IASI moisture and ozone profiles

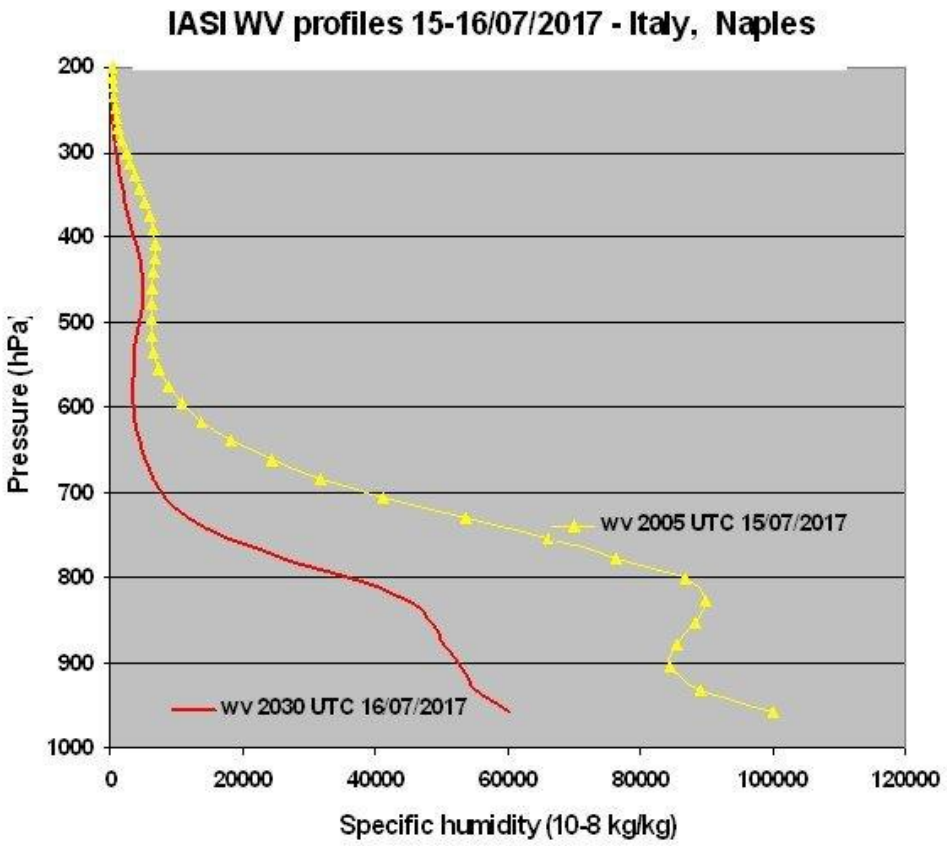

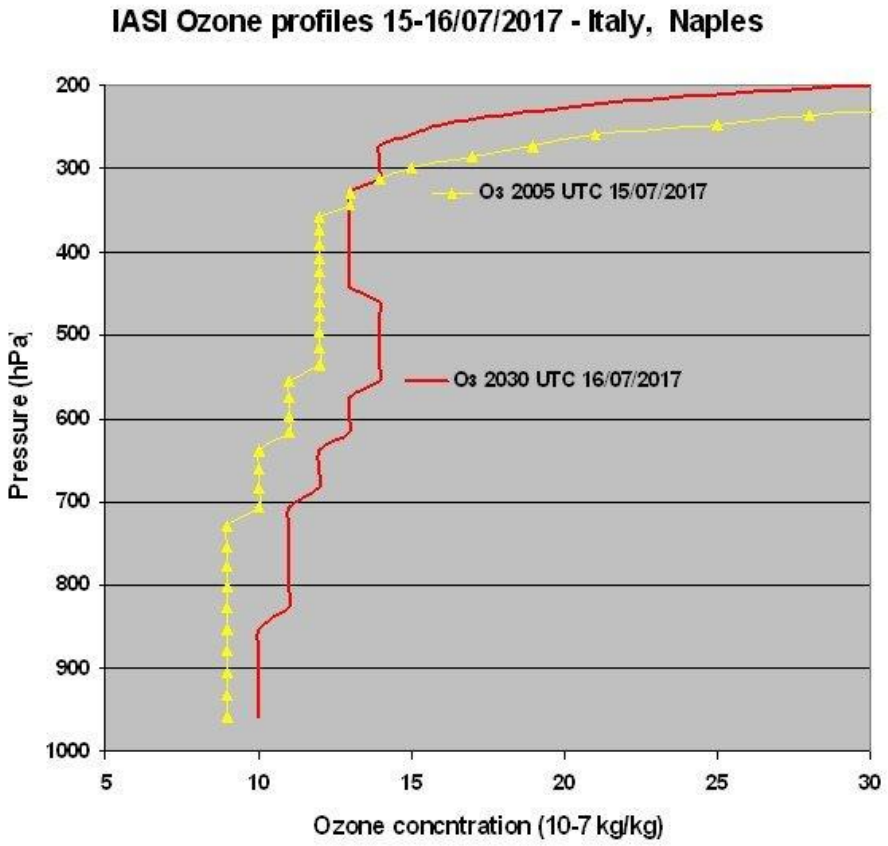

Deep stratospheric dry intrusions may cause significant near-surface air drying and contribute to increase fire activity.

Such a deep stratospheric intrusion is associated with increasing ozone concentration from 300 hPa down to the surface that may be mixed with O_3 production in the fire plume.

Stratospheric intrusion of O3 and production from wildfire

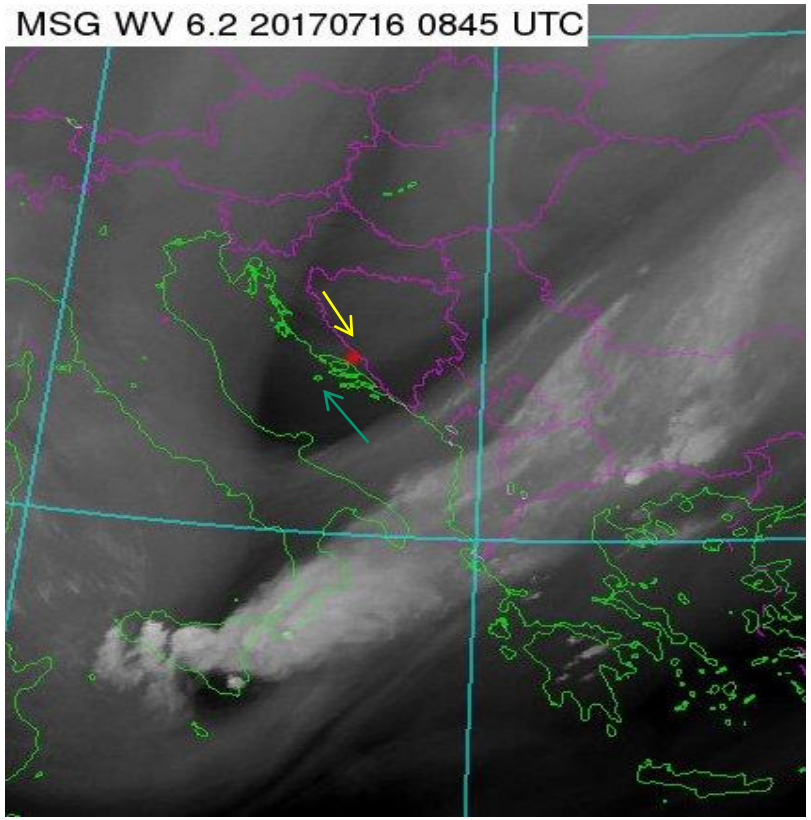

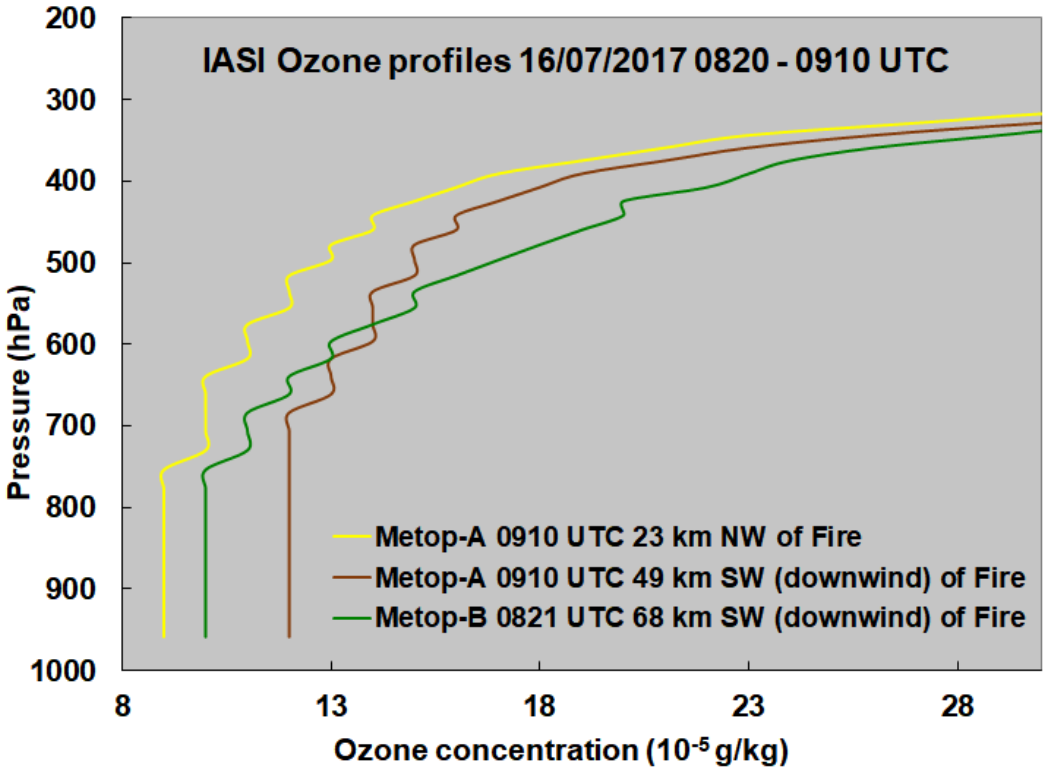

The highest low- mid-level O3 (brown profile) is present 49 km downwind between the green and yellow arrows in the WV imagery, as a result of two mechanisms:

- **Ozone production through photochemical transformations in the fire plume, which has been moving downwind to ~50 km distance for at lest 1.5 hours (first fire detection by FRP at 0745 UTC and wind speed 31.4 km/h, measured in the Split area at 0910 UTC).**
- **Tropopause folding and related subsidence of ozone-rich stratospheric air that seems**
  - **To be acting alone at a longer (68 km) distance 30 min earlier (green profile/arrow)**

No O3 production upwind (NW of Fire, yellow profile) and less stratospheric O3 intrusion (lighter WV image grey shades (yellow arrow) show weaker upper troposphere descent).

Averaged ozone concentration 80 km downwind of wildfires

IASI profiles and FRP help to distinguish the effects of vertical transport of O3 from the O3 production in the fire plume

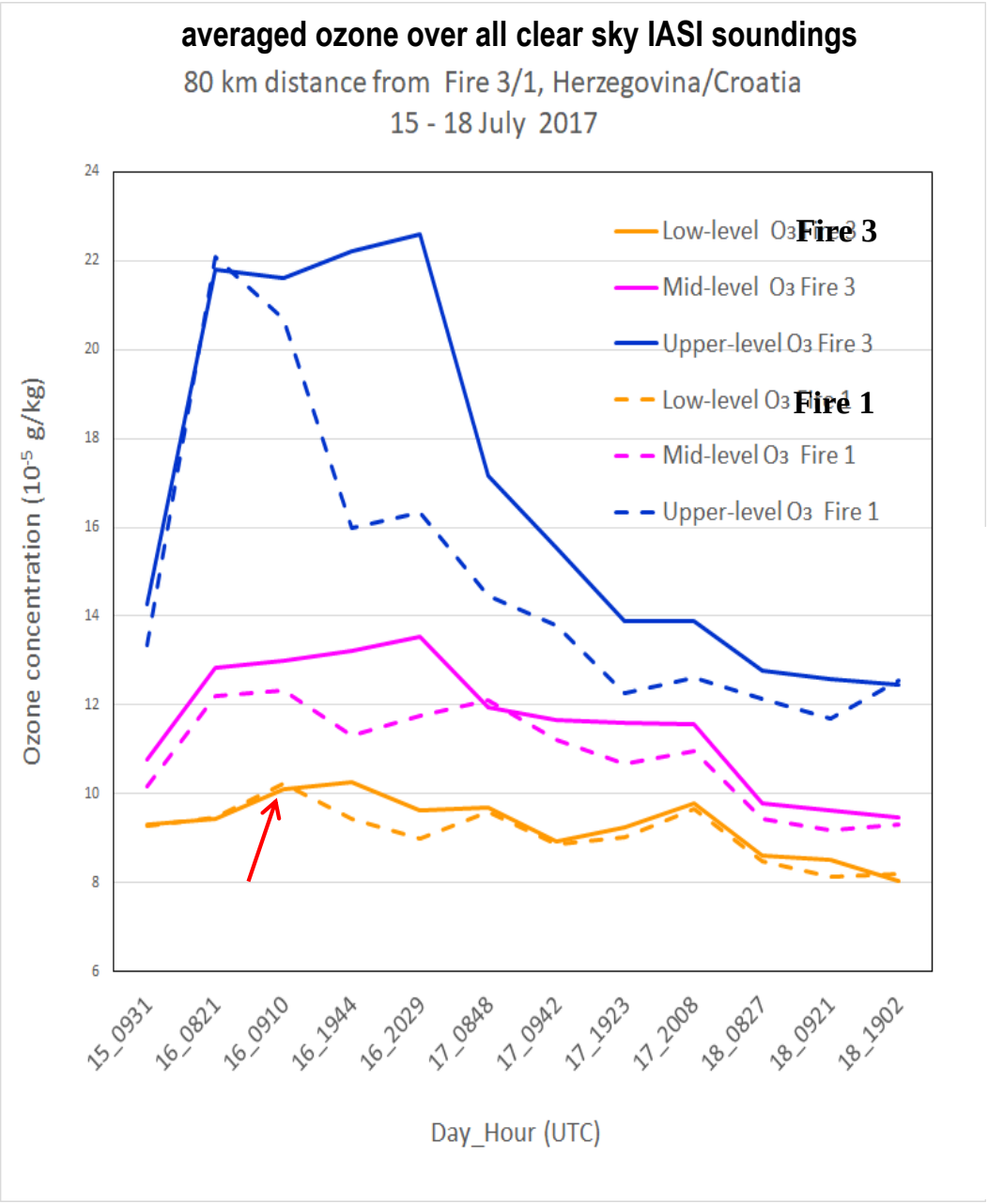

On 16/07/2017 0400 to 0915 UTC, the carbon emission of Fire 1 is much higher than the emission of Fire 3.

Fire	Fire pixels	FRP (MW)	Carbon (kg)
Fire 1	11	2370	366522
Fire 3	19	1035	160022

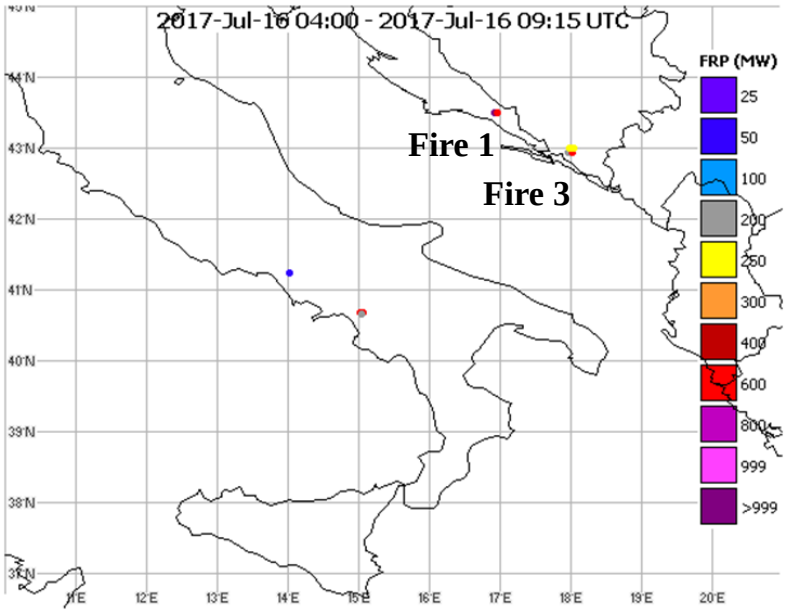

Averaged ozone concentration 80 km downwind of wildfires

IASI profiles and FRP help to distinguish the effects of vertical transport of O3 from the O3 production in the fire plume

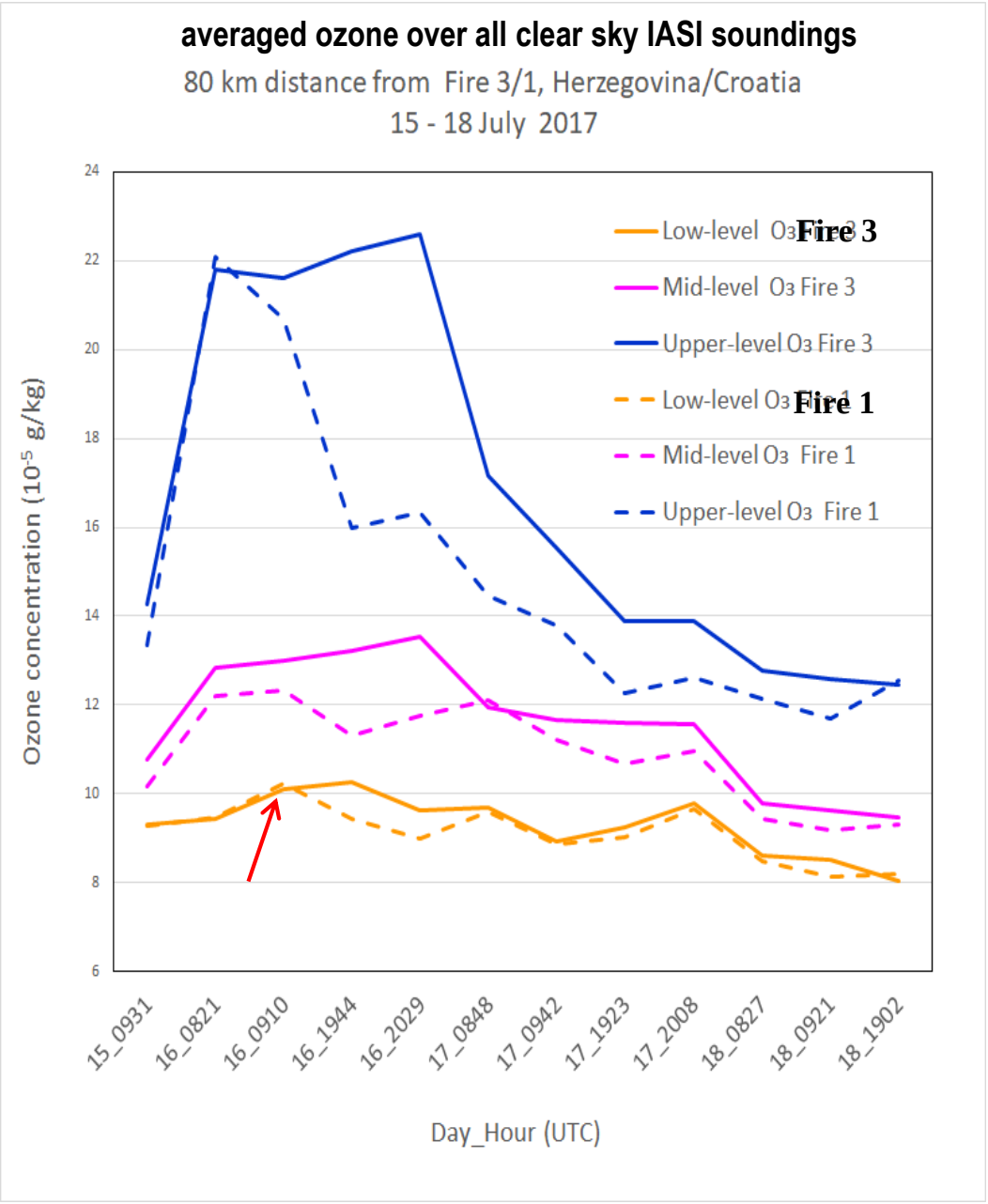

On 16/07/2017 from 0400 to 0915 UTC, the carbon emission of Fire 1 is much higher than the emission of Fire 3.

Fire	Fire pixels	FRP (MW)	Carbon (kg)
Fire 1	11	2370	366522
Fire 3	19	1035	160022

Since ozone and carbon emissions are often correlated in wildfire plumes (Jaffe and Wigder 2012), greater ozone production in the plume of Fire 1 is expected.

Confirmed by IASI measurements:

at 0910 UTC, although in the area of Fire 3, influenced by the stratospheric intrusion, the upper- and mid-level O3 is higher, the low-level ozone in the area of Fire 1 has increased to higher concentrations.

Averaged ozone concentration 80 km downwind of wildfires

WV imagery confirms the effects of vertical transport of O3 from the stratosphere

averaged ozone over all clear sky IASI soundings

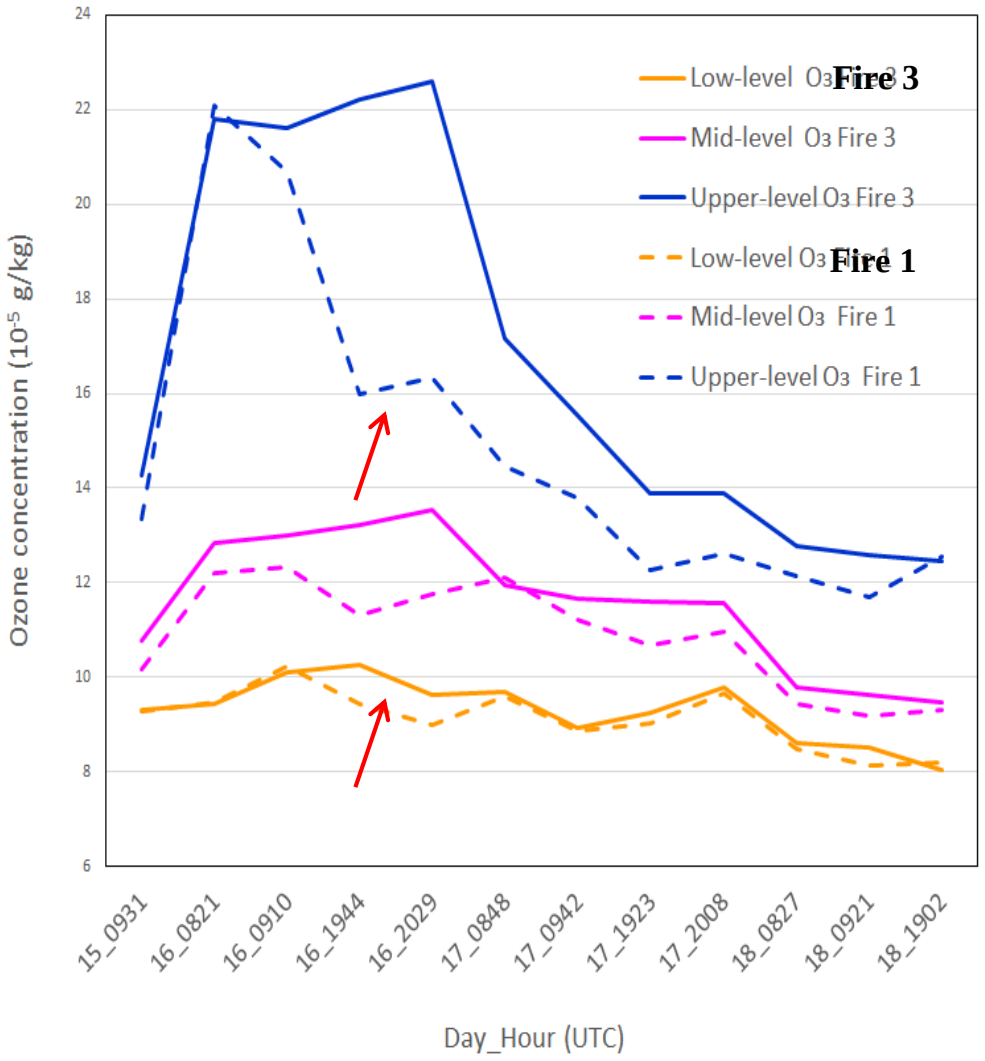

From 16 July afternoon up to 17 July morning low- and mid-level O3 is much higher in Fire 3 area than in the area of Fire 1 due to much stronger stratospheric intrusion there.

Confirmed by MSG WV imagery

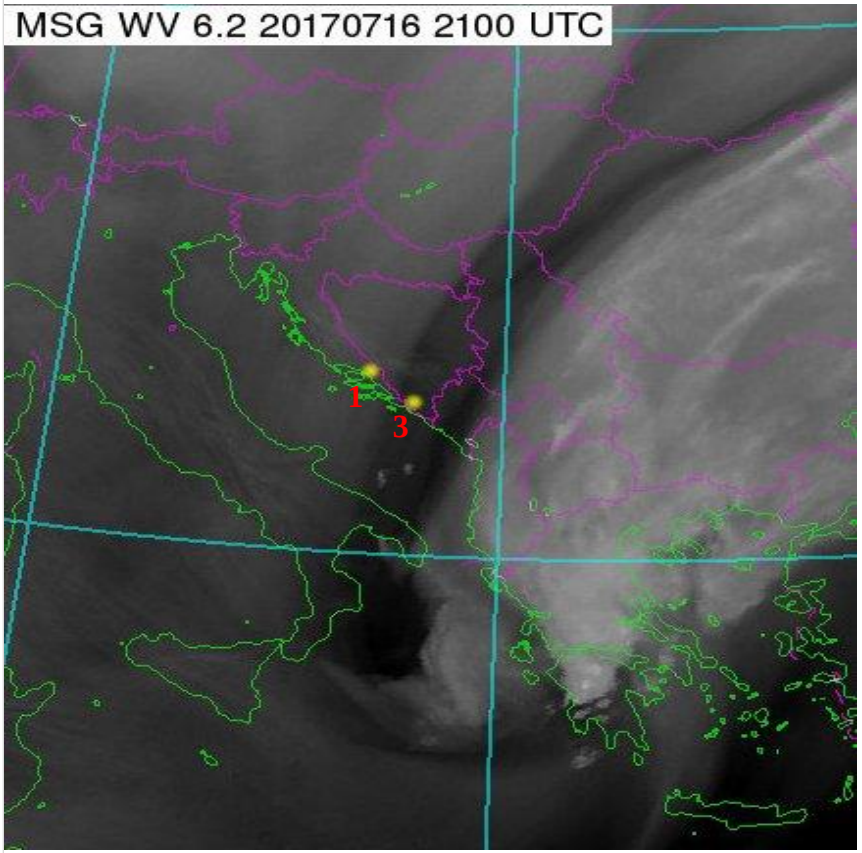

Dry stratospheric intrusion seen in WV imagery and increased fire activity

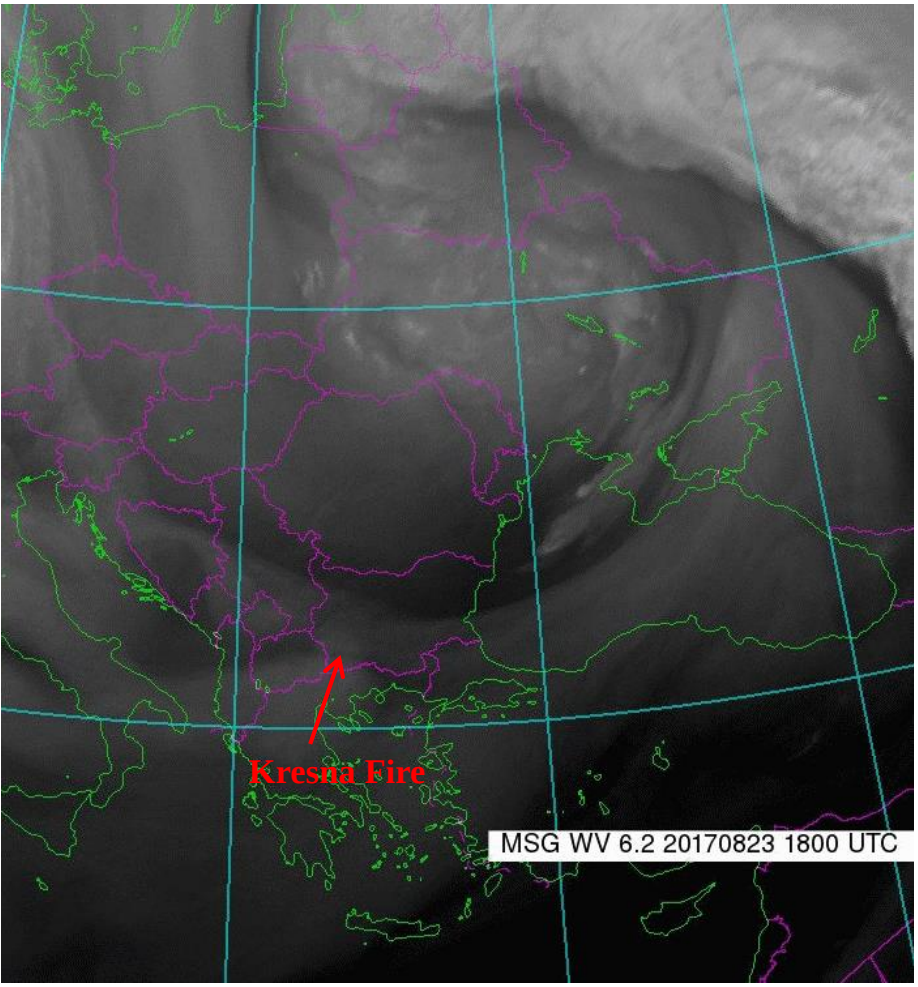

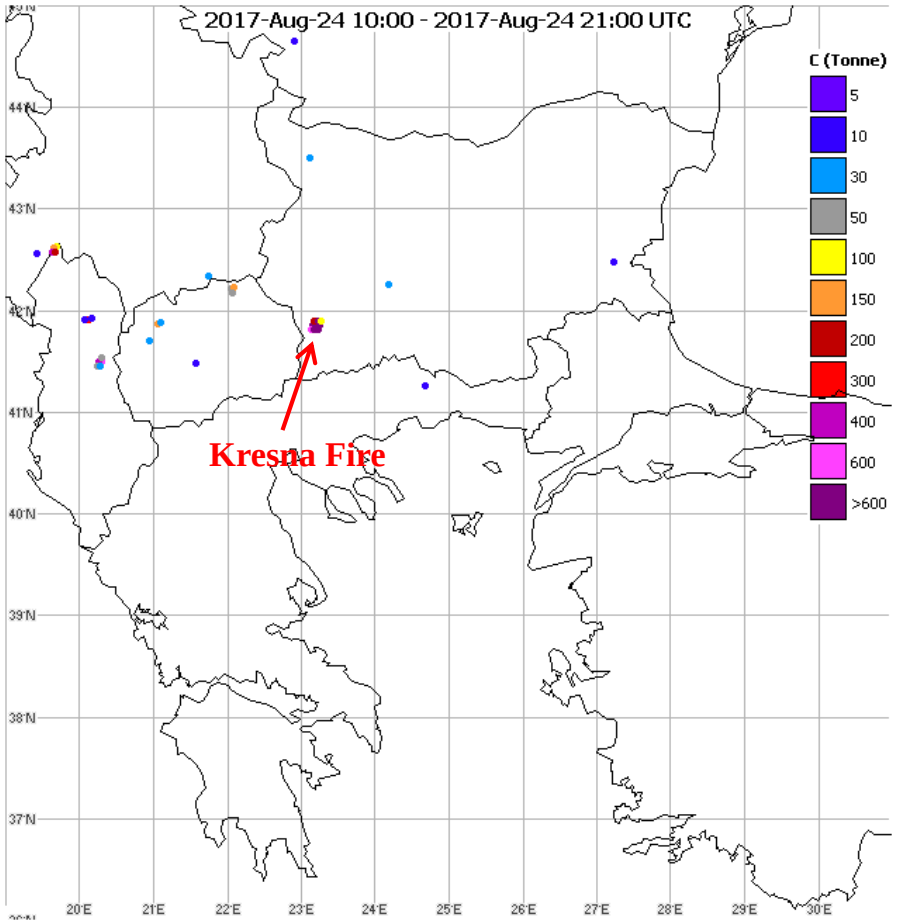

Major wildfire
Kresna, Bulgaria
24 - 29 August 2017

On 24 August 2017 most of the fires detections occurred over the areas affected by the **dry stratospheric intrusion** in Bulgaria, North Macedonia and Albania, although the temperature and humidity conditions over Greece and Turkey are much favourable.

Stratospheric intrusion as a factor for enhanced ozone in the fire area

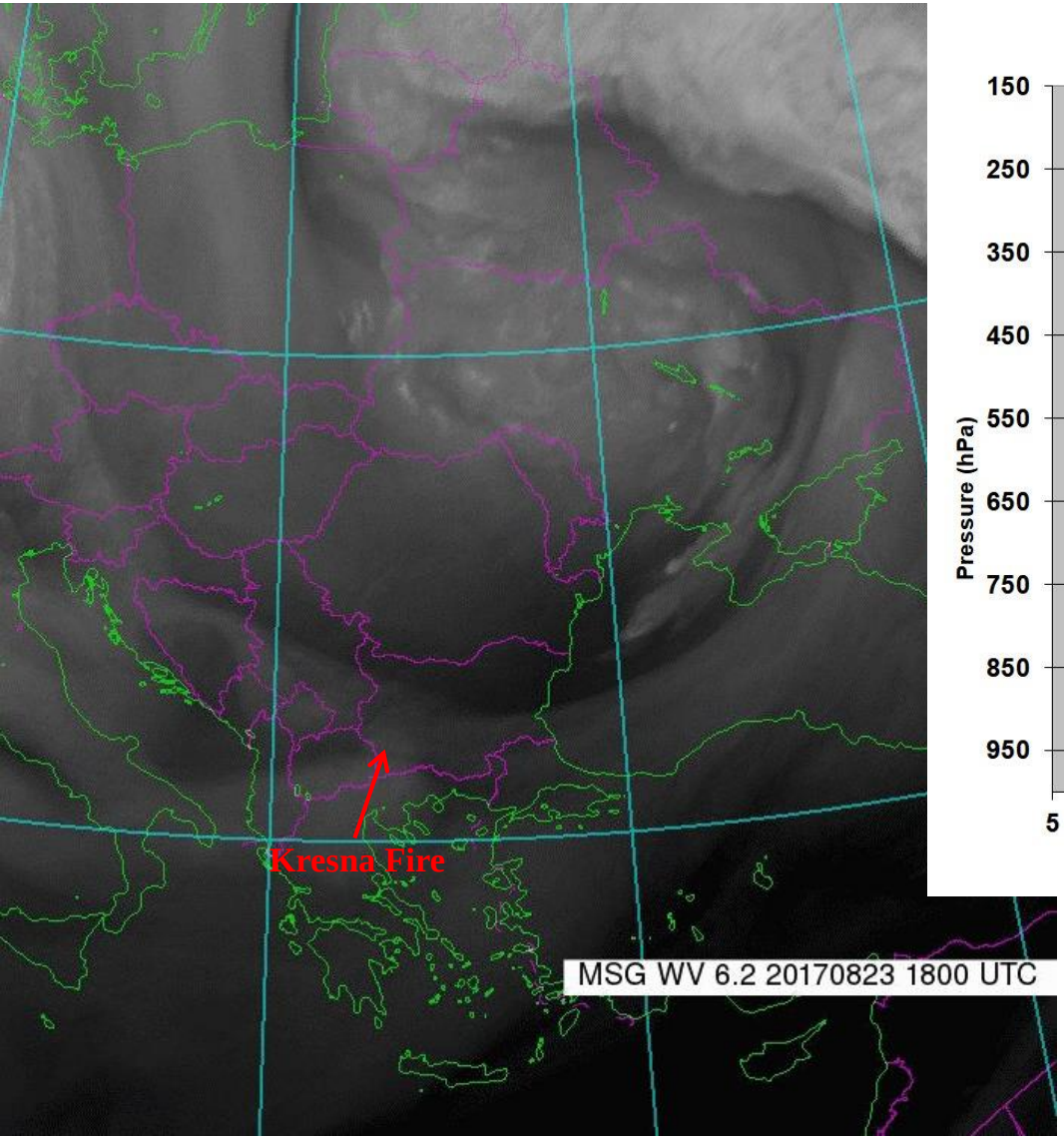

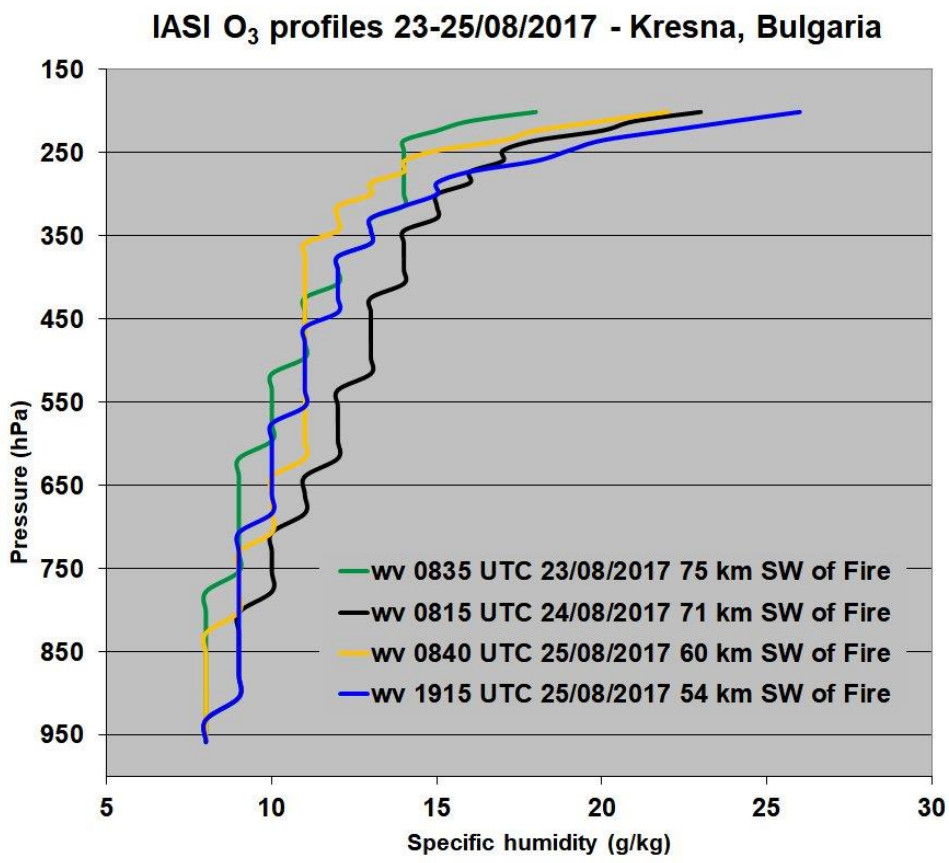

24 August 0900 UTC: Tropopause folding Dynamic Dry zone; Subsidence.

25 August 0900 UTC: Deformation Dry zone; Advection of stratospheric dry air at upper troposphere..

Stratospheric intrusion of ozone and Production of ozone from the wildfire

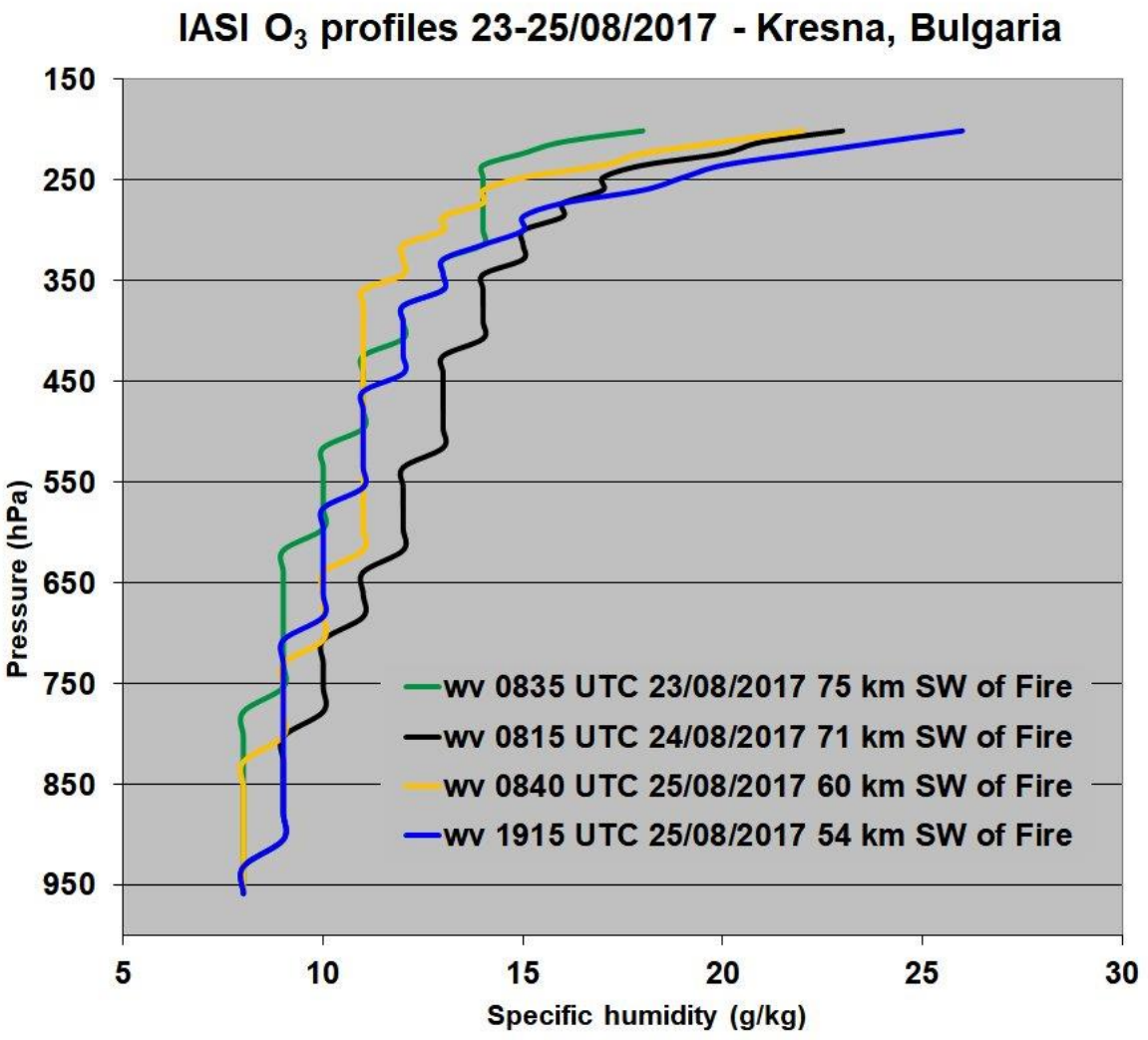

24 August 0815 UTC, ***black profile***

The **stratospheric intrusion of ozone-rich air through subsidence is a significant factor** that contribute to the O3 enhancement over the fire area. Then first Kresna fire detection at 1015 UTC.

25 Aug 0840 UTC, ***yellow profile***

The tropospheric O3 decreased, **no tropopause folding**, ascending motions at upper level.

25 Aug 1915 UTC, ***blue profile***

1. The upper-level ozone increased due to the advection of ozone-rich air. There is **no tropopause folding**, the O3 concentration at mid-level have decreased.

2. At low-level, **O3 production from the wildfire seems to be the main contributing mechanism**.

Satellite detection of Kresna fire, Bulgaria on 24 August 2017

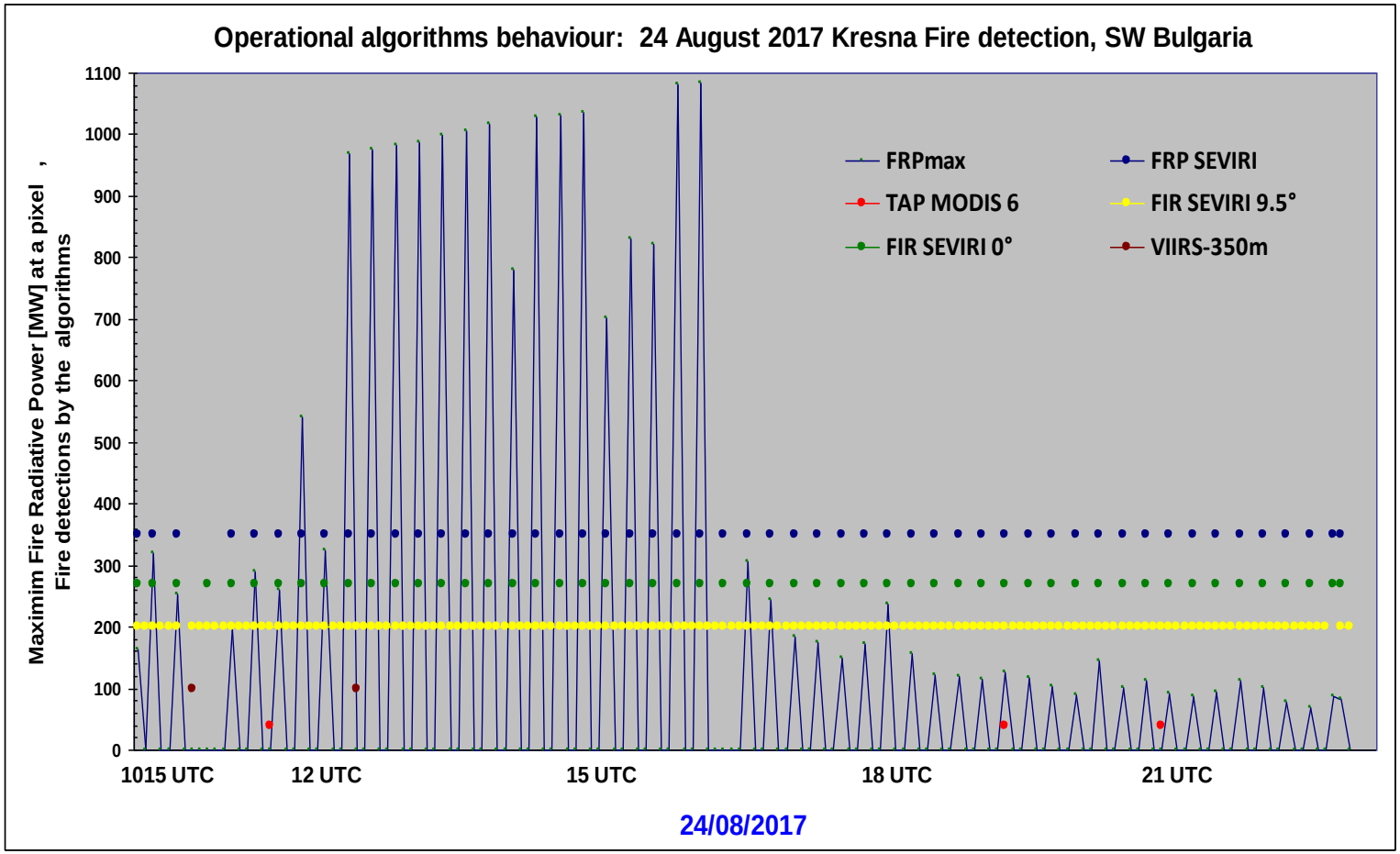

Ozone production from the fire seems to be a significant contributing mechanism for the enhanced low-level O_3 that is confirm by satellite measurements:

- ***FIR Rss: 1015 – 2315 UTC each 15 minutes detections and***
- ***FIR Fss: 1015 – 2330 UTC each 5 minutes (159 time slots) detections***
- ***LSASAF FRP: 1015 – 2315 UTC each 15 minutes detections with 61,586.7 MW radiant energy released and 9,525,640 kg carbon emissions.***
- **MODIS 6 and S-VIIRS also detect the fire**

Wind field evolution as a factor of complexity
Averaged ozone concentration 60/40 km of fire

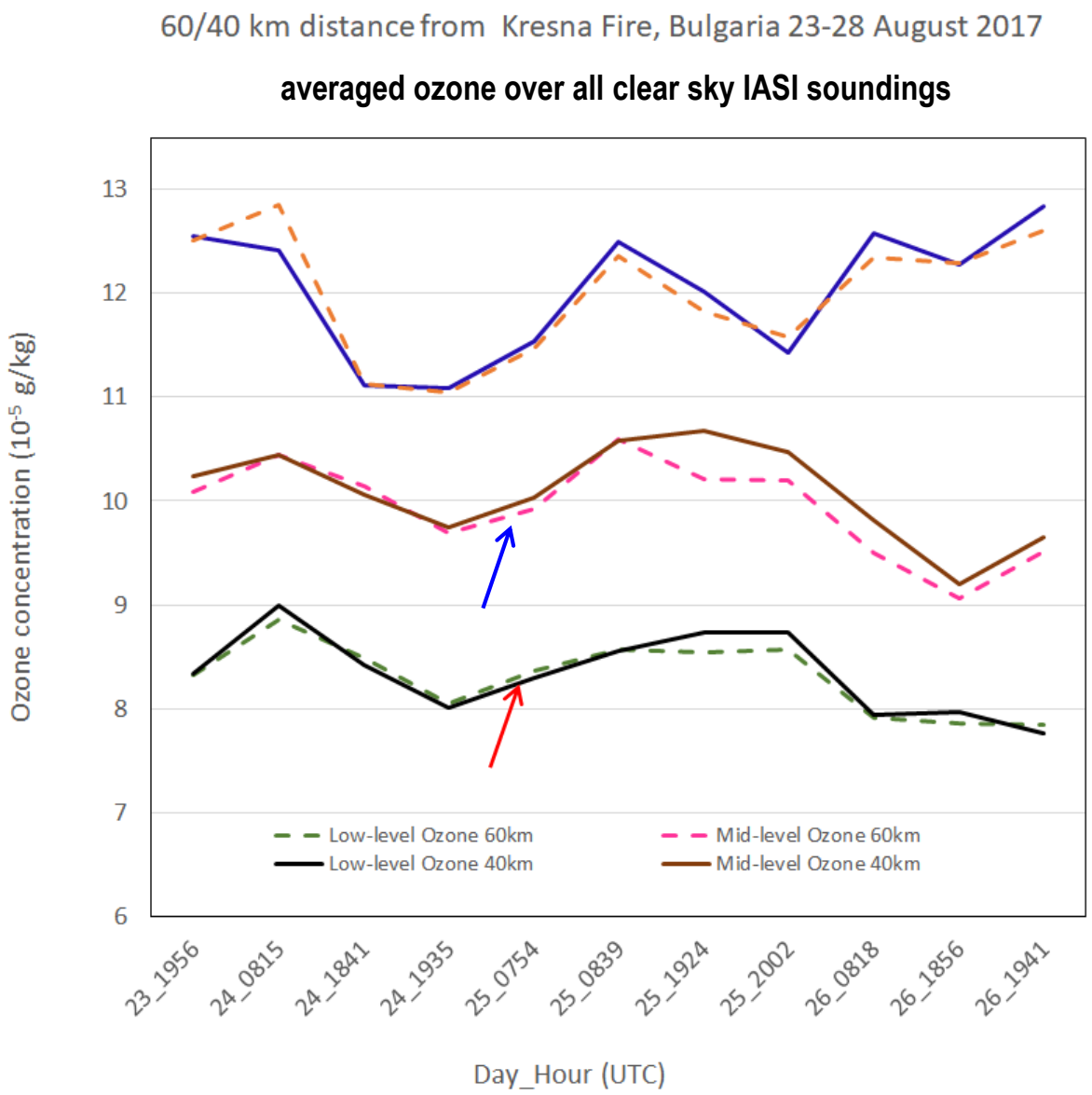

On **24 August**

First fire detection at 1015 UTC.

The O3 is decreasing during the day with the weakening of stratospheric intrusion.

The ozone production from the wildfire can not be distinguished.

On **25 August morning**

The divergent wind over the fire area spreads the fire plume and associated O3 production to a larger distance near the surface.

. Confirmed by IASI profiles:

- At low-level, red arrow the O3 concentration at 60 km distance becomes slightly higher than close to the fire, while
- at mid-level, blue arrow and upper-level, the O3 concentration at 60 km distance is slightly lower.

Wind field evolution as a factor of complexity
Averaged ozone concentration 60/40 km of fire

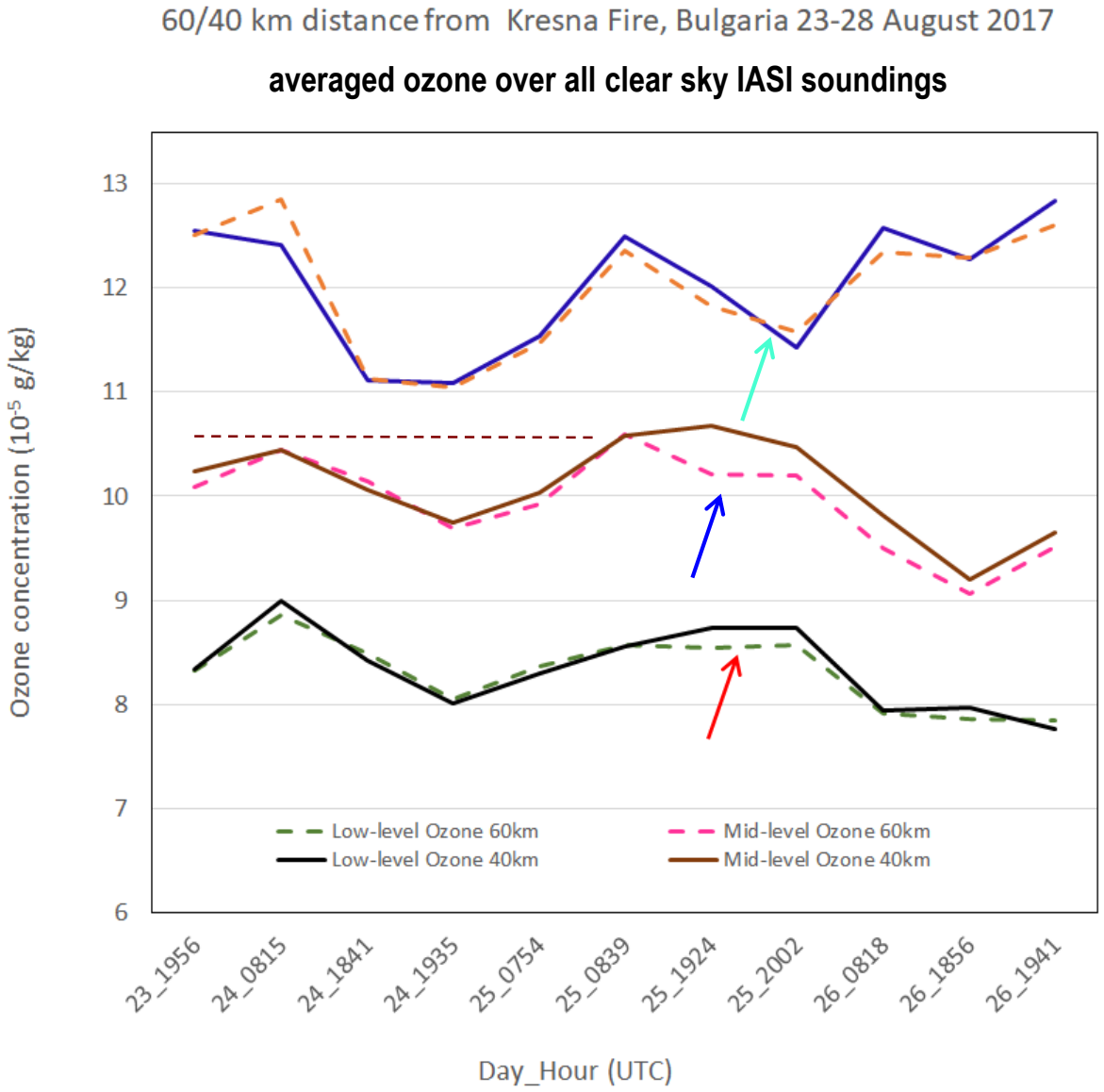

After 1200 UTC on 25 August, the wind changed to a convergent wind field pattern that keeps the plume and produced O3 close to the fire and ascends them to a higher altitude.

Confirmed by IASI profiles:

- At low- and mid-levels the average concentrations of O3 are significantly higher in the area close to the fire (**red** and **blue** arrows).
- At upper-level, **cyan arrow** the O3 concentration at 40 km and 60 km do not differ significantly.

At mid-level, brown dashed line

Higher concentrations on 25 August due to O3 production in the fire plume, although the ozone enhancement from stratospheric intrusion on 24 August was a significant factor.

Conclusion

- Determining the influence of the wildfires on ozone production is complicated as it is combined with the effect of advected and local emissions. At the same time, the most extreme concentrations of ozone coincided with rapidly descending air from midtropospheric levels in areas of tropopause foldings and related stratospheric intrusions.
- Tropospheric profiles retrieved from satellite measurements by IASI instruments are sensitive to increasing low-level ozone concentration in the close vicinity of forest fires in the Central and Eastern Mediterranean.
- The spatial and vertical resolution of soundings from satellite measurements provide a way of efficiently identifying areas of enhanced ozone downwind of wildfires as well as in the environment of a complex wind field.
- IASI profiles, MSG WV imagery and LSASAF FRP help to distinguish the effects of vertical transport of O_3 from the ozone production in the fire plumes.

References

Fox-Hughes P (2015) Characteristics of Some Days Involving Abrupt Increases in Fire Danger. J Appl Meteorol Climatol 54: 2353–2363

Jaffe DA, Wigder NL (2012) Ozone production from wildfires: a critical review. Atmos Environ.;51:1–10. http://dx.doi.org/10.1016/j.atmosenv.2011.11.063.

Mills, Graham, 2008: Abrupt surface drying and fire weather part 2: a preliminary synoptic climatology in the forested areas of southern Australia. Aust. Meteorol. Mag., 57, 311-328.

Rubio MA, Lissi E, Gramsch E, Garreaud RD (2015) Effect of nearby forest fires on ground level ozone concentrations in Santiago, Chile. Atmosphere 6(12): 1926–1938. https://doi.org/10.3390/atmos6121838

Zimet, Tarisa K., Martin J. E., and Potter B. E. (2007). The influence of an upper-level frontal zone on the Mack Lake wildfire environment. Meteorol. Appl., 14, 131-147.